

Figure 3

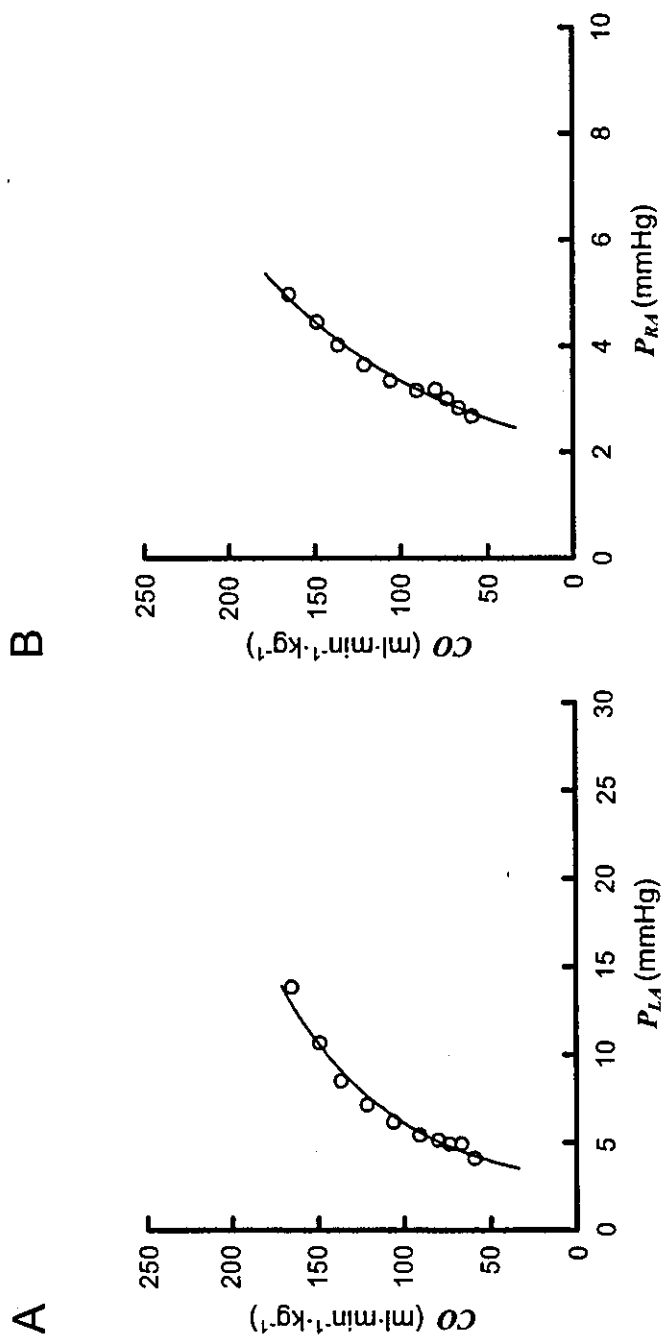


Figure 4

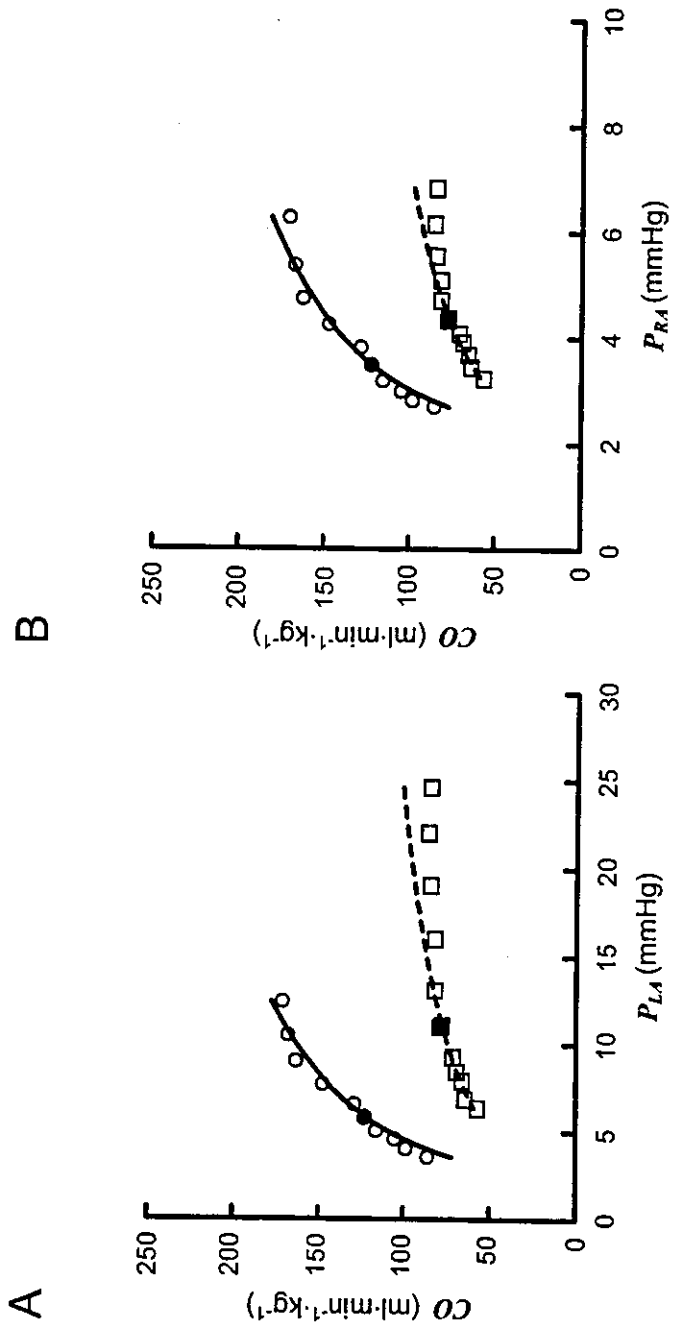
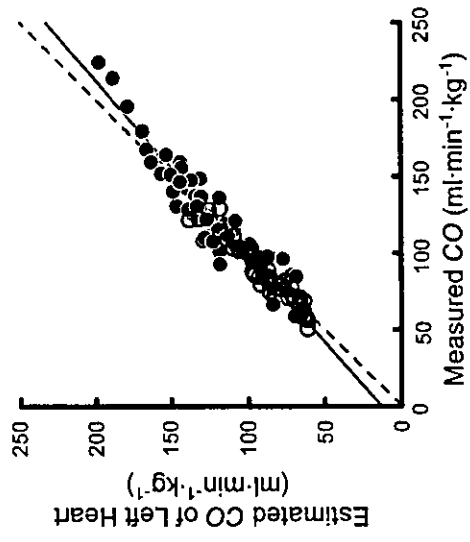


Figure 5

A



B

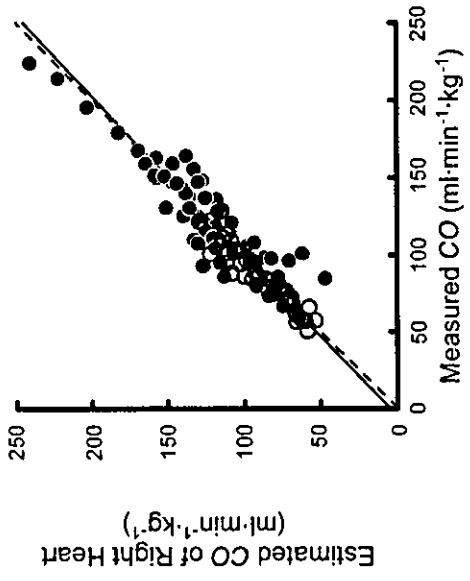
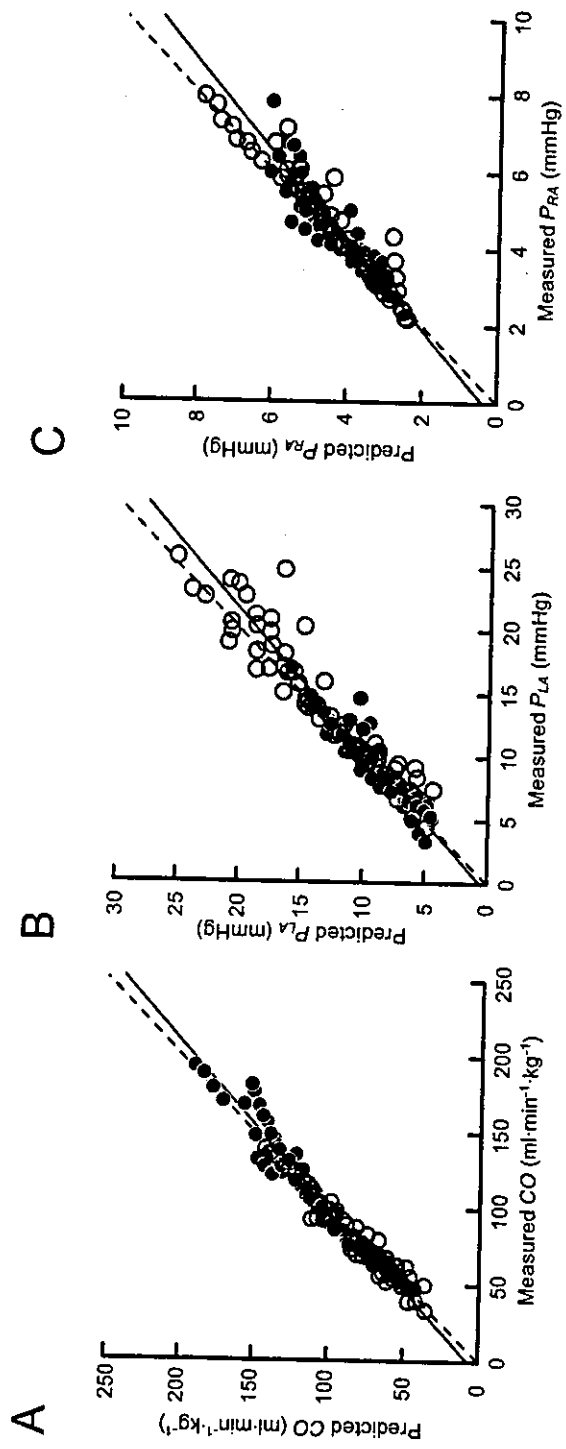


Figure 6



Cellular and Ionic Mechanism for Drug-Induced Long QT Syndrome and Effectiveness of Verapamil

Takeshi Aiba, MD, PhD,* Wataru Shimizu, MD, PhD,† Masashi Inagaki, MD,*
Takashi Noda, MD, PhD,* Shunichiro Miyoshi, MD, PhD,‡ Wei-Guang Ding, MD, PhD,§
Dimitar P. Zankov, MD,§|| Futoshi Toyoda, PhD,§ Hiroshi Matsuura, MD, PhD,§
Minoru Horie, MD, PhD,|| Kenji Sunagawa, MD, PhD*

Osaka, Tokyo, and Shiga, Japan

OBJECTIVES	We examined the cellular and ionic mechanism for QT prolongation and subsequent Torsade de Pointes (TdP) and the effect of verapamil under conditions mimicking <i>KCNQ1</i> (I_{Ks} gene) defect linked to acquired long QT syndrome (LQTS).
BACKGROUND	Agents with an I_{Kr} -blocking effect often induce marked QT prolongation in patients with acquired LQTS. Previous reports demonstrated a relationship between subclinical mutations in cardiac K^+ channel genes and a risk of drug-induced TdP.
METHODS	Transmembrane action potentials from epicardial (EPI), midmyocardial (M), and endocardial (ENDO) cells were simultaneously recorded, together with a transmural electrocardiogram, at a basic cycle length of 2,000 ms in arterially perfused feline left ventricular preparations.
RESULTS	The I_{Kr} block (E-4031: 1 $\mu\text{mol/l}$) under control conditions ($n = 5$) prolonged the QT interval but neither increased transmural dispersion of repolarization (TDR) nor induced arrhythmias. However, the I_{Kr} blocker under conditions with I_{Ks} suppression by chromanol 293B 10 $\mu\text{mol/l}$ mimicking the <i>KCNQ1</i> defect ($n = 10$) preferentially prolonged action potential duration (APD) in EPI rather than M or ENDO, thereby dramatically increasing the QT interval and TDR. Spontaneous or epinephrine-induced early afterdepolarizations (EADs) were observed in EPI, and subsequent TdP occurred only under both I_{Ks} and I_{Kr} suppression. Verapamil (0.1 to 5.0 $\mu\text{mol/l}$) dose-dependently abbreviated APD in EPI more than in M and ENDO, thereby significantly decreasing the QT interval, TDR, and suppressing EADs and TdP.
CONCLUSIONS	Subclinical I_{Ks} dysfunction could be a risk of drug-induced TdP. Verapamil is effective in decreasing the QT interval and TDR and in suppressing EADs, thus preventing TdP in the model of acquired LQTS. (J Am Coll Cardiol 2005;45:300-7) © 2005 by the American College of Cardiology Foundation

The long QT syndrome (LQTS) is characterized by a prolongation of ventricular repolarization and recurrent episodes of atypical polymorphic ventricular tachycardia known as Torsade de Pointes (TdP) leading to sudden cardiac death (1-3). The molecular basis of congenital LQTS is attributed to defects in several ion channel genes encoding delayed rectifier K^+ or Na^+ currents. On the other hand, agents that block rapidly activating delayed rectifier potassium current (I_{Kr}) often induce marked QT prolongation with an inverted T wave in patients with acquired LQTS. Recent studies indicate that some cases of drug-induced LQTS can be associated with silent mutations and common polymorphism in genes responsible for the congenital LQTS (4), such as *KCNQ1* encoding slowly

activating delayed rectifier potassium currents (I_{Ks}) (5-7). However, it remains unclear why subclinical I_{Ks} dysfunction is a risk of drug-induced LQTS.

Both early afterdepolarization (EAD)-induced triggered activity and increased dispersion of repolarization have been suggested as important in the genesis of ventricular arrhythmias in congenital and acquired LQTS. Moreover, verapamil, an L-type Ca^{2+} channel blocker, suppressed EADs and TdP in patients with LQTS (8,9). In the present study, we hypothesized that: 1) addition of I_{Kr} block to I_{Ks} dysfunction markedly prolongs action potential duration (APD) and induces TdP by producing EADs and/or increases transmural dispersion of repolarization (TDR); and 2) verapamil suppresses TdP by preventing EADs and decreasing TDR. In arterially perfused feline left ventricular wedge preparations, we demonstrated that subclinical I_{Ks} dysfunction, mimicking *KCNQ1* defect, could be a risk of drug-induced TdP, and verapamil successfully suppressed TdP in the model of acquired LQTS.

METHODS

Arterially perfused wedge preparations and electrophysiologic recordings. All animal care procedures were in accordance with the position of the American Heart Association research animal use (November 11, 1984). The

From the *Department of Cardiovascular Dynamics, Research Institute, and †Division of Cardiology, Department of Internal Medicine, National Cardiovascular Center, Suita, Osaka, Japan; the ‡Department of Physiology, Keio University School of Medicine, Tokyo, Japan; §Department of Physiology and ||Department of Cardiovascular and Respiratory Medicine, Shiga University of Medicine, Otsu, Shiga, Japan. This study was supported by the Program for Promotion of Fundamental Studies in Health Science of the Organization for Pharmaceutical Safety and Research (of Japan) (to Dr. Sunagawa), a grant from the Japan Cardiovascular Research Foundation (to Dr. Aiba), Fukuda Foundation for Medical Technology (to Dr. Inagaki), Vehicle Racing Commemorative Foundation (to Dr. Shimizu), Health Sciences Research Grants from the Ministry of Health, Labour and Welfare (to Dr. Shimizu), and the Research grant for Cardiovascular Disease (15C-6) from the Ministry of Health, Labour and Welfare (to Dr. Shimizu).

Manuscript received August 24, 2004; revised manuscript received September 21, 2004, accepted September 28, 2004.

Abbreviations and Acronyms

APD ₉₀	= action potential duration measured at 90% repolarization
BCL	= basic cycle length
EAD	= early afterdepolarization
I _K	= delayed rectifier potassium current
I _{Kr}	= rapidly activating delayed rectifier potassium current
I _{Ks}	= slowly activating delayed rectifier potassium current
LQTS	= long QT syndrome
TdP	= Torsade de Pointes
TDR	= transmural dispersion of repolarization

methods used for isolation, perfusion, and recording of transmembrane activity from the arterially perfused feline left ventricle have been detailed in a previous study (10) and are similar to methods reported using canine or rabbit wedge preparations (11-15). Briefly, a transmural wedge was dissected from the anterior wall of the left ventricle, cannulated via the left descending coronary artery (or the first branch of the left circumflex), and placed in a small tissue bath arterially perfused with Tyrode's solution. The temperature was maintained at $37 \pm 1^\circ\text{C}$ and perfusion pressure maintained between 40 and 60 mm Hg. Ventricular wedges were stimulated with bipolar electrodes applied to the endocardial surface. We recorded a transmural electrocardiogram (ECG) (epicardial, positive pole) using Ag-AgCl electrodes, and transmembrane action potentials (APs) simultaneously from the epicardium, midmyocardium (M), and endomyocardium using three separate intracellular floating microelectrodes. The epicardial and endocardial APs were recorded from the epicardial and endocardial surfaces, respectively, at positions approximating the transmural axis of the ECG. The M-cell's AP was recorded from the transmural surface, mainly at the subendocardium, along the same axis.

An I_{Kr} blocker, E-4031 $1 \mu\text{mol/l}$, was used in control condition ($n = 5$) or under condition with I_{Ks} suppression by chromanol 293B $10 \mu\text{mol/l}$, mimicking *KCNQ1* defect ($n = 10$). The effects of an L-type Ca²⁺ channel blocker, verapamil, were evaluated at 0.1, 1, 2.5, and $5 \mu\text{mol/l}$ under the I_{Ks} and I_{Kr} suppression (acquired LQTS condition). Epinephrine $0.5 \mu\text{mol/l}$ was used to mimic increased sympathetic activity in the absence and presence of verapamil under the acquired LQTS condition. The spontaneous or epinephrine-induced EADs and subsequent TdP were evaluated under each set of conditions.

Data using E-4031, 293B, 293B + E-4031, and additional verapamil on top of 293B + E-4031 were collected for a period of 30 min starting 30 min after applying the above compounds to the perfusion. The APD was measured at 90% repolarization (APD₉₀). The TDR was defined as the difference between the longest and shortest repolarization times (activation time + APD₉₀) of the APs recorded across the wall. The QT interval was defined as the time

interval between the QRS onset and the point at which the line of maximal downslope of the positive T wave and the line of the maximal upslope of the negative T wave crossed the baseline.

Whole-cell patch-clamp experiments. Epicardial, M, and endocardial cells isolated from the feline left ventricle were voltage-clamped using whole-cell configuration of the patch-clamp technique (16). Patch electrodes were pulled from borosilicate glass capillaries, heat-polished, and had a tip resistance of 2.0 to 3.0 M Ω when filled with standard pipette solution containing (mmol/l): 70 potassium aspartate, 50 KCl, 10 KH₂PO₄, 1 MgSO₄, 3 Na₂-ATP, 0.1 Li₂-GTP, 5 EGTA, and 5 HEPES (pH adjusted to 7.2 with KOH). Membrane currents were recorded from the epicardial, M, and endocardial cells superfused at 34 to 36°C with normal Tyrode's solution containing (mmol/l): 140 NaCl, 5.4 KCl, 1.8 CaCl₂, 0.5 MgCl₂, 0.33 NaH₂PO₄, 5.5 glucose, and 5.0 HEPES (pH adjusted to 7.4 with NaOH). In all current measurements, nisoldipine ($0.4 \mu\text{mol/l}$) was added to normal Tyrode's solution to abolish I_{Ca,L}. The cell membrane capacitance (C_m) was calculated for each cell by fitting the single exponential function to the decay of the capacitive transient elicited by a 5-mV step hyperpolarization applied from a holding potential of -50 mV (17).

Simulation study. Isolated epicardial, M, and endocardial cells were simulated using a Luo-Rudy dynamic cell model modified by varying the maximum conductance (density) of I_{Kr} and I_{Ks} (G_{Kr} and G_{Ks}) as described previously (18), in which the G_{Ks}/G_{Kr} in the epicardial, M, and endocardial cells were 23, 17, and 19, respectively. The transient outward potassium current (I_{to}) was incorporated into the model using the formulation of Dumaine et al. (19), in which the maximum conductance of I_{to} (G_{to}) was set to 0.5, 0.25, and 0.05 mS/ μF in the epicardial, M, and endocardial cells, respectively.

Statistics. Statistical analysis of the data was performed with a Student *t* test for paired data or analysis of variance coupled with Bonferroni's test, as appropriate. Data are expressed as mean values \pm SD except for those shown in the figures, which are expressed as mean \pm SEM. Significance was defined as a value of $p < 0.05$.

RESULTS

The QT interval, APD, and TDR under an acquired LQTS condition with or without epinephrine. Figure 1 shows transmembrane activity recorded simultaneously from the epicardium, M, and endocardium together with a transmural ECG at a basic cycle length (BCL) of 2,000 ms. E-4031 ($1 \mu\text{mol/l}$) alone significantly, but homogeneously, prolonged APD of the three regions, causing no major change in TDR (Fig. 1B). Chromanol 293B ($10 \mu\text{mol/l}$) alone did not significantly increase the QT interval, APD of the three regions, and TDR (Fig. 1C). The additional E-4031 to 293B, mimicking acquired LQTS, preferentially prolonged epicardial APD, thus dramatically increased QT

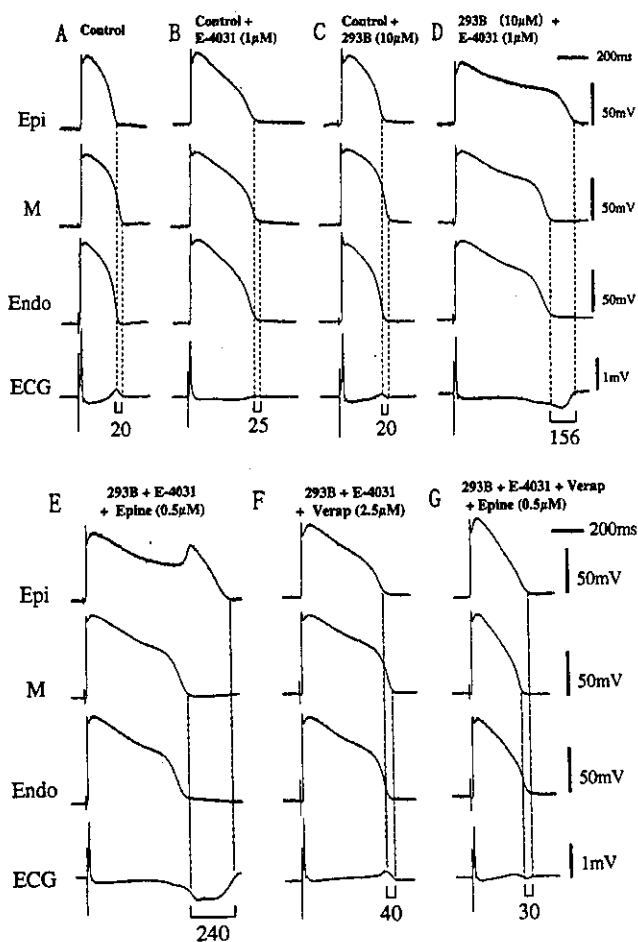


Figure 1. Transmembrane action potentials simultaneously recorded from the epicardial (Epi), midmyocardial (M), and endocardial (Endo) regions and a transmural electrocardiogram (ECG) at basic cycle length of 2,000 ms under each study condition. (A) Control. (B) E-4031 (1 μ M). (C) Chromanol 293B (10 μ M). (D) 293B + E-4031 (acquired long QT syndrome [LQTS] condition). (E) Epinephrine infusion (Epine: 0.5 μ M) under acquired LQTS condition. (F) Addition of verapamil (Verap) 2.5 μ M under acquired LQTS condition. (G) Further addition of Epine in the continued presence of Verap under acquired LQTS condition. Numbers at bottom of each ECG denote transmural dispersion of repolarization (ms).

interval and TDR (Fig. 1D). Epinephrine infusion (0.5 μ M) further prolonged epicardial APD associated with induction of EADs, but did not prolong M or endocardial

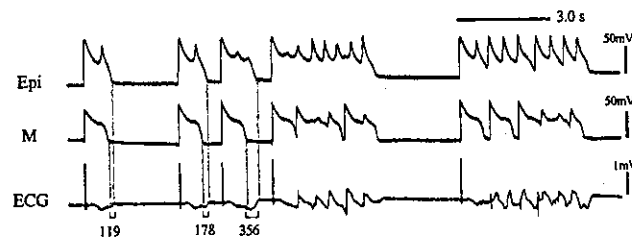


Figure 2. Spontaneous early afterdepolarization and subsequent Torsade de Pointes under the acquired long QT syndrome condition (293B 10 μ M + E-4031 1 μ M). Basic cycle length = 3,000 ms. Recordings and abbreviations as in Figure 1.

APD, resulting in further QT prolongation and increasing TDR (Fig. 1E).

The composite data of the QT interval, APD₉₀ of the epicardium, M, and endocardium, and TDR at a BCL of 2,000 ms are shown in Table 1. E-4031 under control significantly, but homogeneously, prolonged APD₉₀, resulting in neither change of TDR nor induction of arrhythmia. Chromanol 293B under control did not significantly increase APD₉₀ of the three regions, resulting in no major change in QT interval and TDR. Whereas additional E-4031 to 293B markedly prolonged QT interval as evidenced by preferential prolongation of the epicardial APD₉₀ compared with M and endocardial APD₉₀, thus dramatically increased TDR. Epinephrine further prolonged the epicardial APD₉₀, but shortened the M region APD₉₀, resulting in further prolongation of the QT interval and increasing TDR.

Neither E-4031 alone nor 293B alone produced any EADs or TdP. However, additional E-4031 to 293B (acquired LQTS condition) induced spontaneous EADs from the epicardium in 5 of 10 preparations, including two preparations with spontaneous TdP (Fig. 2), but not from the M or endocardium. Further epinephrine infusion (n = 8) induced EADs from the epicardium in all preparations, including four preparations with subsequent TdP, but EADs from the M region were seen in only one preparation.

Effect of verapamil on the QT interval, APD, TDR, and induction of arrhythmias under an acquired LQTS condition. Under the acquired LQTS condition, verapamil dose-dependently (0.1 to 5 μ M) abbreviated APD of

Table 1. Effect of I_{Kr} Block With or Without Pretreated I_{Ks} Block on the QT Interval, APD₉₀, and Transmural Dispersion of Repolarization

	QT	APD ₉₀			TDR
		Epi	M	Endo	
Control (n = 5)	283 ± 15	227 ± 16	259 ± 8	246 ± 13	31 ± 10
E-4031 (1 μ M) (n = 5)	446 ± 42*	373 ± 30*	408 ± 28*	374 ± 25*	34 ± 4
Control (n = 10)	279 ± 12	230 ± 16	253 ± 14	237 ± 19	24 ± 5
293B (10 μ M) (n = 10)	298 ± 34	252 ± 26	275 ± 33	253 ± 16	24 ± 9
293B (10 μ M) + E-4031 (1 μ M) (n = 10)	793 ± 183*	723 ± 164*	596 ± 131*	545 ± 78*	175 ± 68*
293B + E-4031 + Epine (0.5 μ M) (n = 8)	866 ± 251	801 ± 217	506 ± 123	525 ± 118	191 ± 75
293B + E-4031 + Verap (2.5 μ M) (n = 7)	557 ± 178†	503 ± 171†	483 ± 135†	516 ± 154	35 ± 37†
293B + E-4031 + Verap + Epine (n = 6)	445 ± 113†	403 ± 117†	399 ± 93†	411 ± 98†	30 ± 12†

*p < 0.001 vs. control, †p < 0.05 vs. 293B + E-4031; ‡p < 0.01 vs. 293B + E-4031 by analysis of variance with Bonferroni's test.

APD₉₀ = action potential duration at 90% repolarization; Endo = endocardium; Epi = epicardium; Epine = epinephrine; I_{Ks} = slowly activating delayed rectifier potassium current; I_{Kr} = rapidly activating delayed rectifier potassium current; M = mid-myocardium; QT = QT interval; TDR = transmural dispersion of repolarization; Verap = verapamil.

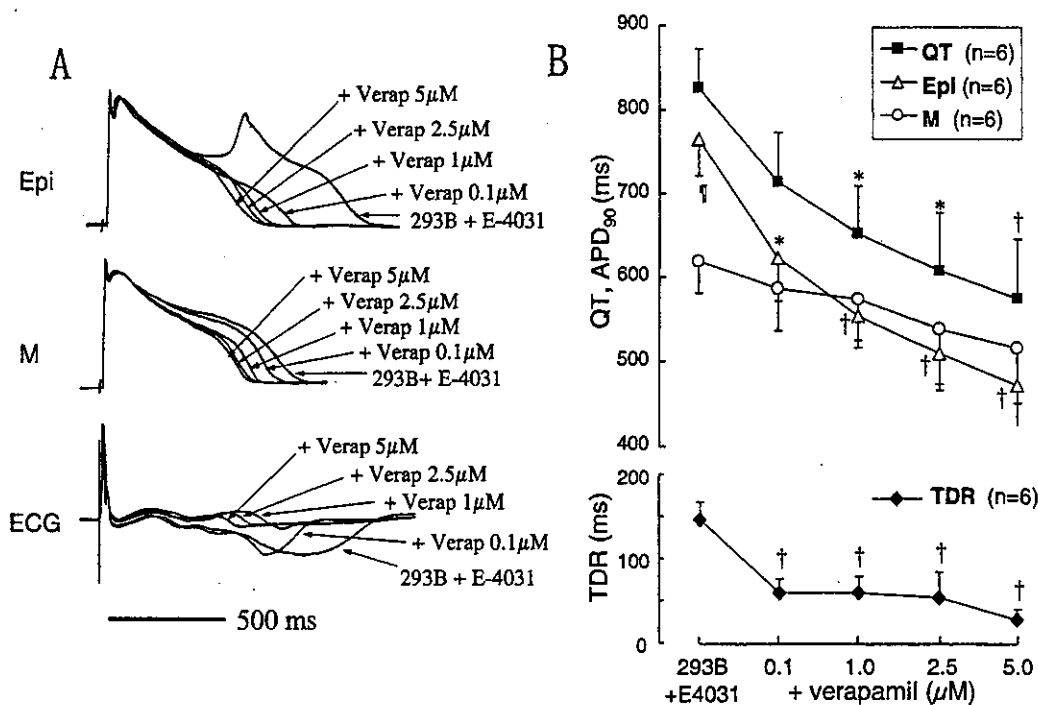


Figure 3. Dose-dependent effect of Verap (0.1 to 5 $\mu\text{mol/l}$) on transmembrane and ECG activity under acquired LQTS condition (293B 10 $\mu\text{mol/l}$ + E-4031 1 $\mu\text{mol/l}$). (A) Superimposed action potentials recorded simultaneously from the epicardial and M regions together with a transmural ECG. (B) Composite data of the effect of Verap on QT interval (solid squares), action potential duration measured at 90% repolarization (APD₉₀) of Epi (open triangles) and M (open circles) regions and transmural dispersion of repolarization (TDR) (solid diamonds). Basic cycle length = 2,000 ms. * $p < 0.05$ vs. 293B + E-4031; † $p < 0.01$ vs. 293B + E-4031; ‡ $p < 0.05$ vs. M region by analysis of variance with Bonferroni's test. Abbreviations as in Figure 1.

the epicardial and M regions as well as the QT interval (Fig. 3A). Figure 3B shows composite data of the dose-dependent effect of verapamil on the QT interval, APD₉₀ of the epicardial and M regions, and TDR under the acquired LQTS condition (n = 6). A 5- $\mu\text{mol/l}$ dose of verapamil under the acquired LQTS condition preferentially abbreviated the epicardial APD₉₀ (761 \pm 99 ms to 469 \pm 95 ms; $p < 0.001$) compared with the M region APD₉₀ (615 \pm 83 ms to 512 \pm 146 ms; $p = \text{NS}$), resulting in a significant decrease in TDR (146 \pm 46 ms to 26 \pm 28 ms; $p < 0.01$). The change in QT interval paralleled the decrease in the epicardial APD₉₀.

As shown in Figure 1F, 2.5- $\mu\text{mol/l}$ verapamil preferentially abbreviated the epicardial APD₉₀ rather than the M or endocardium, thus significantly abbreviated QT interval and TDR. Moreover, verapamil completely prevented the influence of epinephrine in inducing EADs and TdP as well as increasing the epicardial APD₉₀, QT interval, and TDR (Fig. 1G). The composite data of the effect of verapamil on the QT interval, APD, and TDR with or without epinephrine are shown in Table 1. Thus, verapamil totally suppressed EADs and TdP under the acquired LQTS condition with or without epinephrine.

Measurement of I_{Kr} and I_{Ks} in epicardial, M, and endocardial cells. Figure 4A represents the dose-dependent inhibition of I_{Ks} by 293B in an epicardial cell. Figure 4B illustrates the concentration-response relation-

ships for the inhibition of I_{Ks} tail current. The data points were reasonably well described by a Hill equation with the following parameters: IC₅₀ = 6.39 \pm 1.17 $\mu\text{mol/l}$, n_H = 1.23 \pm 0.05 (epicardial cells: n = 5); IC₅₀ = 5.71 \pm 1.32 $\mu\text{mol/l}$, n_H = 1.25 \pm 0.12 (M cells: n = 5); IC₅₀ = 5.73 \pm 0.94 $\mu\text{mol/l}$, n_H = 1.07 \pm 0.19 (endocardial cells: n = 5). There are no significant differences in IC₅₀ and n_H values among the epicardial, M, and endocardial cells (analysis of variance with Bonferroni's test), thus indicating that I_{Ks} in these three cell types represents a similar sensitivity to inhibition by chromanol 293B.

Figure 5 represents the sensitivity of I_K to blockers of I_{Kr} and I_{Ks} (E-4031 and 293B, respectively). After the I_K reached a practically steady level (control, trace 1), application of E-4031 (3 $\mu\text{mol/l}$) markedly reduced the amplitude of I_K tail current (trace 2), and further addition of 293B (30 $\mu\text{mol/l}$) almost completely abolished the I_K tail current (trace 3). Table 2 summarizes densities of I_{Kr} and I_{Ks} in the epicardial, M, and endocardial cells, determined as E-4031- and 293B-sensitive tail currents normalized with reference to C_m. In each cell type, the density of I_{Ks} was significantly smaller than that of I_{Kr}. The density of I_{Kr} was almost equivalent among the three cell types, whereas I_{Ks} density was significantly smaller in M cells compared with that in the epicardial and endocardial cells.

Computer simulations. To understand why EAD developed from the epicardium under the acquired LQTS

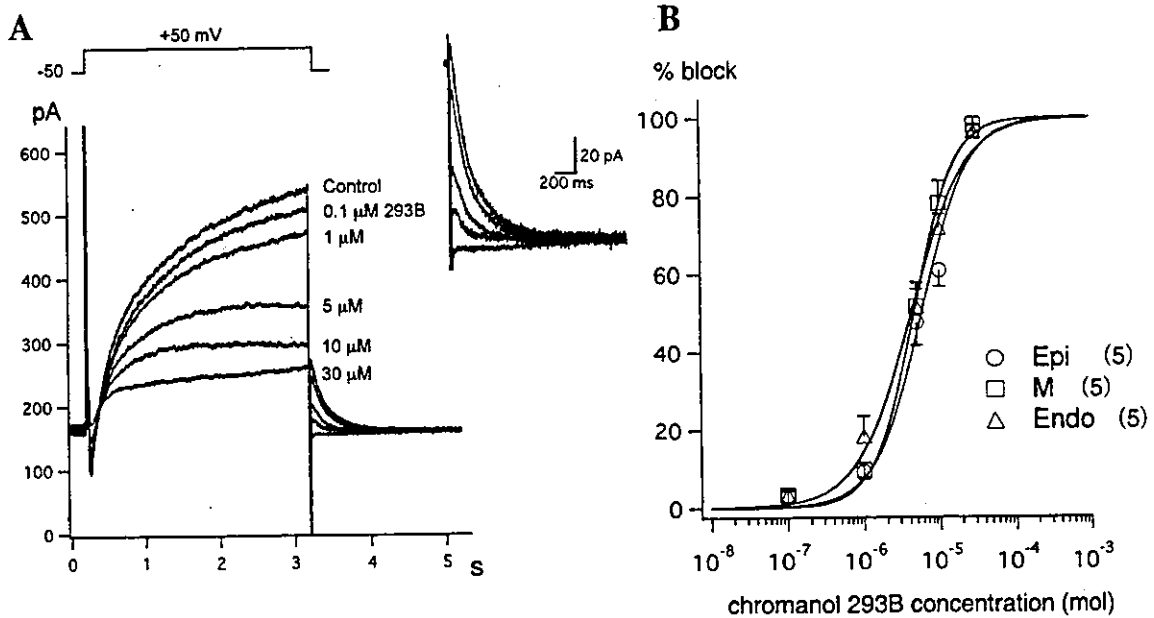


Figure 4. Sensitivity of I_{Ks} in the epicardial (Epi), midmyocardial (M), and endocardial (Endo) cells to inhibition by chromanol 293B. (A) Representative superimposed current traces elicited by 3-s depolarizing voltage-clamp steps applied from a holding potential of -50 mV to $+50$ mV in an epicardial cell, before (control) and during exposure to 293B at a concentration of 0.1, 1, 5, 10, and 30 $\mu\text{mol/l}$. The I_{Ks} inhibitor E-4031 (3 $\mu\text{mol/l}$) was present throughout. Tail currents were demonstrated on an expanded scale. (B) The percent block of I_{Ks} in the Epi (open circles), M (open squares), and Endo (open triangles) cells. The degree of I_{Ks} inhibition was measured as the fraction of the tail current reduced by each concentration of 293B with reference to the control amplitude of the tail current. Smooth curves through the data points represent a least-squares fit of a Hill equation: percent block = $100/(1 + (IC_{50}/[293B])^{n_H})$, yielding the concentration required for the half-maximal block (IC_{50}) and the Hill coefficient (n_H). pA = pico ($\times 10^{-12}$) Ampere.

condition, we simulated APs of the three cell types using a Luo-Rudy model at a BCL of 2,000 ms. As shown in Figure 6A, the epicardial APD was shorter than the M cells under the control condition (dotted line). However, suppression of both I_{Kr} and I_{Ks} (70% and 80%, respectively) (solid line), simulating the condition of acquired LQTS, developed

EAD (arrow) from the epicardial cell but not from M or endocardial cells. Moreover, Figure 6B shows that the reactivation of Ca^{2+} current through the L-type channel (I_{CaL}) was responsible for the development of epicardial EAD under the acquired LQTS condition. Furthermore, a decrease in I_{to} density changed by G_{to} from 0.5 to 0.05

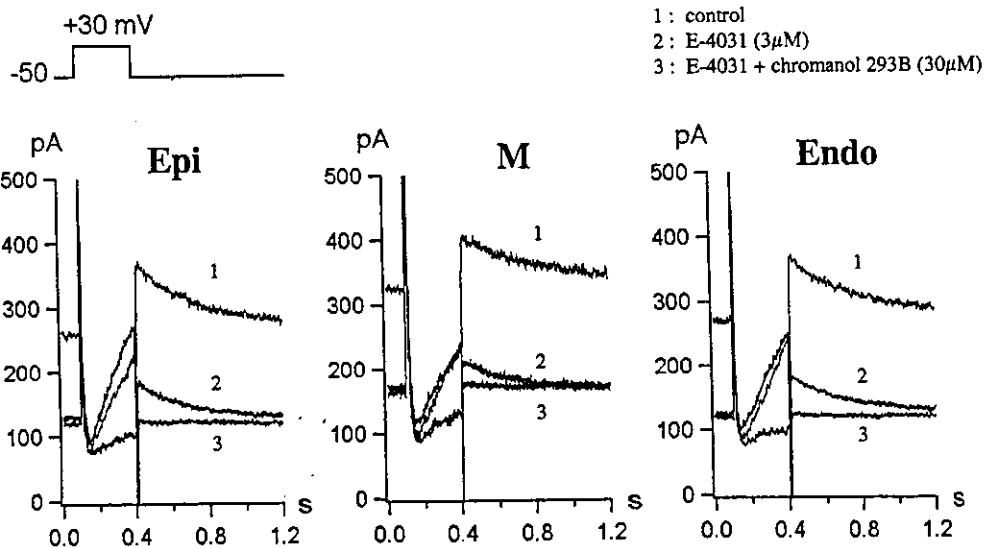


Figure 5. Detection of I_{Kr} and I_{Ks} in the epicardial (Epi), midmyocardial (M), and endocardial (Endo) cells. Depolarizing test pulses (to $+30$ mV for 300 ms) were repetitively applied (every 2 s) from a holding potential of -50 mV to activate I_{Ks} , and membrane currents were recorded from the Epi, M, and Endo cells, before (trace 1), and ~ 2 min after exposure to 3 $\mu\text{mol/l}$ E-4031 (trace 2), and ~ 2 min after further addition of 30 $\mu\text{mol/l}$ 293B in conjunction with 3 $\mu\text{mol/l}$ E-4031 (trace 3). pA = pico ($\times 10^{-12}$) Ampere.

Table 2. Transmural Heterogeneity of I_{Ks} and I_{Kr} in Feline Left Ventricle

	Epi (n = 10)	M (n = 9)	Endo (n = 7)
I_{Ks}	$0.35 \pm 0.26^*$	$0.13 \pm 0.09^{*†}$	$0.30 \pm 0.09^*$
I_{Kr}	1.34 ± 0.51	1.10 ± 0.38	1.17 ± 0.30

* $p < 0.05$ vs. I_{Kr} ; † $p < 0.05$ vs. Epi and Endo by analysis of variance with Bonferroni's test. Mean \pm SD, (pA/pF). Current densities of I_{Kr} and I_{Ks} measured as E-4031- and chromanol 293B-sensitive tail currents at -50 mV. Abbreviations as in Table 1.

mS/ μ F decreased the net charge entry carried by the $I_{Ca,L}$ during the AP, resulted in suppressing EAD as well as abbreviating APD.

DISCUSSION

Genetic and ionic substrates of acquired LQTS. Acquired QT prolongation and TdP arrhythmias usually require multiple risk factors, such as bradycardia, hypokalemia, female gender, and mostly agents with an I_{Kr} -blocking effect. Recent genetic studies suggest some forms of acquired LQTS can be associated with silent mutations in the LQTS-related genes (4), such as *KCNQ1* encoding I_{Ks} (so-called forme fruste type of congenital LQTS) (5-7). Roden (20) hypothesized "reduced repolarization reserve" as a potential mechanism underlying susceptibility to drug-induced LQTS. According to his hypothesis, I_{Ks} dysfunction could be potentially compensated by other K^+ currents, mainly I_{Kr} , thereby the repolarization defect is tolerated, and agents with I_{Kr} block could induce acquired QT prolongation and TdP.

Vos et al. (21-23) suggested a high incidence of EADs and TdP by *d*-sotalol in dogs with chronic complete atrioventricular block as a result of a significant down-regulation of I_{Ks} and I_{Kr} . Moreover, other experimental studies using canine and rabbit wedge showed combined I_{Ks} and I_{Kr} block caused a high incidence of EADs most likely arising from the epicardium (14,15). Burashnikov and Antzelevitch (24) suggested that the abundant I_{Ks} in the epicardium and endocardium compared with the M region under normal conditions contributed to the increase in TDR but protected against development of EADs in the epicardium and endocardium in dogs. Thus, I_{Ks} is critically important for the repolarization reserve in the epicardium and endocardium.

Although I_{Ks} in the feline heart is far smaller than that in other species (25,26), our result from a whole-cell patch-clamp study suggested that a $10\text{-}\mu\text{mol/l}$ 293B used in the wedge preparation reduced about 70% of I_{Ks} in the three cell types, which is consistent with degree of I_{Ks} blockade caused by a silent mutation or common polymorphism in human *KCNQ1* gene (6,7). We also showed that I_{Kr} block with E-4031 in control conditions prolonged the QT interval but did not increase TDR and developed neither EADs nor TdP. However, combined I_{Kr} block with 293B further prolonged the QT interval and inverted T wave, which, in turn, increased TDR and induced EADs and TdP. There-

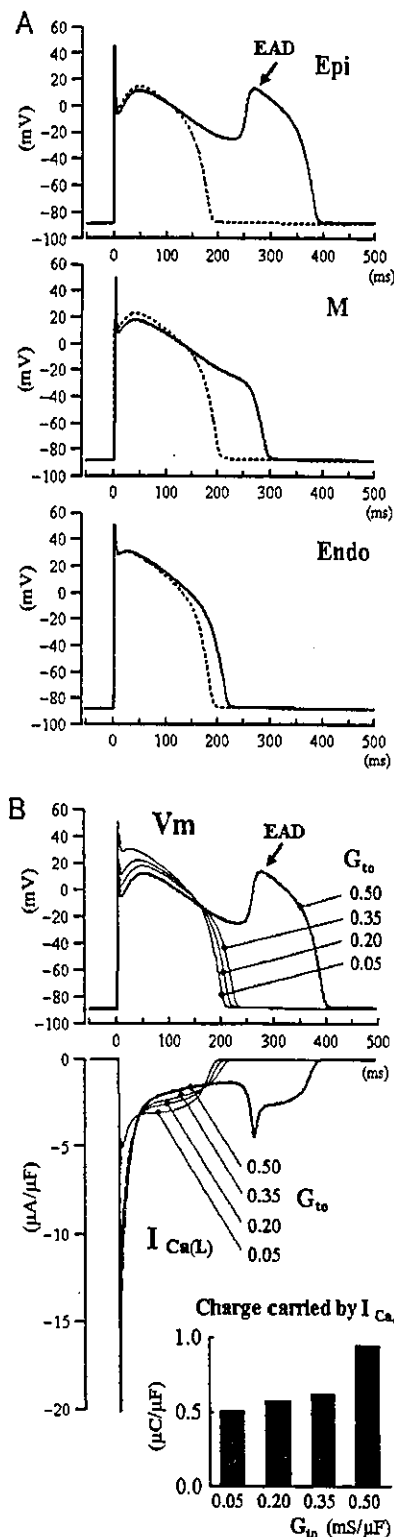


Figure 6. Effect of both I_{Kr} and I_{Ks} suppression on the simulated action potentials from the epicardial (Epi), midmyocardial (M), and endocardial (Endo) cells. (A) Superimposed action potentials simulated under baseline condition (dotted lines) and after both I_{Kr} and I_{Ks} suppression (70% and 80%, respectively) (solid lines). (B) Effect of maximum conductance of I_{Ks} (G_{to}) on the simulated epicardial action potential (V_m), $I_{Ca,L}$ magnitude, and the net charge entry calculated by integration of the $I_{Ca,L}$ under the condition of both I_{Kr} and I_{Ks} suppression. Basic cycle length = 2,000 ms. EAD = early afterdepolarization.

fore, the feline heart is appropriate for a model of forme fruste LQTS. Our data also suggested that subclinical I_{K_s} dysfunction may become a genetic substrate, and additional I_{K_r} suppression may unmask marked QT prolongation and TdP in acquired form of LQTS.

Role of $I_{Ca,L}$ in increasing TDR and inducing EADs and TdP in acquired LQTS. Several clinical and experimental studies have suggested that EADs and triggered activity were important in the genesis of QT prolongation and TdP in LQTS (8,9,11-15,22-24). Induction of EADs generally requires an initiation or conditioning phase controlled by the sum of membrane currents present at the plateau AP (inward depolarization current and outward repolarization current). January and Riddle (27) suggested that the time- and voltage-dependent $I_{Ca,L}$ within its "window" was important in the induction and block of EADs. Luo and Rudy (28) suggested that EADs resulted from a secondary activation of the $I_{Ca,L}$ during the plateau of AP. However, the mechanism responsible for a high incidence of EADs (especially from the epicardium) and subsequent TdP under conditions of severely eliminated outward K^+ current, mimicking acquired LQTS, has not been mechanistically defined.

Our data indicate that accentuation of $I_{Ca,L}$ during the AP plateau preferentially prolonged APD and triggered EADs in the epicardium. This was based on the effect of verapamil on the epicardium. However, it is still unclear whether a larger $I_{Ca,L}$ in the epicardial cell compared with the M or endocardial cells contributed to the development of EADs. Recently, Bányász et al. (29) reported in their AP voltage clamp experiments that the epicardial cell had a pool of Ca^{2+} channels sufficient for a second activation, whereas the endocardial cells did not. Cordeiro et al. (30) also noted that the presence of spike-and-dome AP waveform in the epicardial cells resulted in a greater magnitude of $I_{Ca,L}$. Moreover, several simulation studies demonstrated a strong coupling between $I_{Ca,L}$ and I_{to} (31,32). Our simulation study also suggested that larger I_{to} in the epicardial cell caused larger $I_{Ca,L}$, developing EADs under the acquired LQTS condition. In the feline left ventricle, it has been reported that I_{to} is larger in the epicardium compared with the endocardium (33). Therefore, larger $I_{Ca,L}$ secondary to I_{to} -mediated spike-and-dome AP configuration in the epicardial cell might be responsible for the high incidence of EADs from the epicardium. This does not necessarily exclude the possible mechanisms of other ionic currents such as I_{NaCa} and Ca^{2+} release from sarcoplasmic reticulum, which may contribute to the prolonged AP as well as to the development of EADs under calcium-loading conditions (34).

Effects of catecholamines and verapamil in acquired LQTS. Treatment of drug-induced TdP begins with immediate withdrawal of any potential drugs and risk factors. Sanguinetti et al. (35) suggested that an increase of heart rate by isoproterenol was an effective therapeutic strategy in patients with acquired LQTS, because beta-adrenergic

stimulation with isoproterenol abbreviates repolarization not only by increasing heart rate, but also by directly increasing the magnitude of I_{K_s} . However, our experimental data shows that epinephrine further prolonged APD in the epicardium and induced EADs and TdP probably due to augmentation of $I_{Ca,L}$ in the acquired LQTS condition. Thus, beta-adrenergic stimulation could be arrhythmogenic even in conditions of acquired LQTS when subclinical I_{K_s} dysfunction is present and heart rate is not fully increased.

Cosio et al. (8) used intravenous verapamil to treat three patients with TdP during an atrioventricular block. Shimizu et al. (9) reported that verapamil suppressed spontaneous or epinephrine-induced EADs and TdP in patients with congenital LQTS. Experimentally, Kimura et al. (36) reported that verapamil (2 $\mu\text{mol/l}$) suppressed cocaine-induced EADs in the myocytes isolated from feline left ventricle. Taken together with the data in the present study, $I_{Ca,L}$ block with verapamil may be a therapeutic choice for TdP in patients with acquired LQTS as well as congenital LQTS.

Study limitations. We assumed the activity recorded from the cut surface of the perfused wedge preparation represented cells within the respective layers of the wall throughout the wedge. Such validation was provided in previous studies that used the wedge preparation (10-15).

Pharmacologic block of I_{K_s} with 293B is not a complete surrogate for *KCNQ1* defect. However, our feline model closely mimicked the degree of I_{K_s} inhibition and pharmacologic features of acquired LQTS. Therefore, we believe these qualitative similarities validate 293B as a surrogate for forme fruste LQTS.

We simulated APs of the three cell types using a Luo-Rudy model, but it does not completely represent feline ventricular APs. However, the phenomenon that EAD frequently developed from the epicardium under the acquired LQTS condition was observed not only in cats but also in dogs and rabbits (14,15); thus, this simulation may support our speculation about the mechanism of this phenomenon.

Finally, the concentration of verapamil mainly used in this study (2.5 $\mu\text{mol/l}$ = 1,250 ng/ml) was considerably higher than a typical clinical dose. However, verapamil was effective in suppressing EADs and decreasing TDR even at the lowest dose used in this study (0.1 $\mu\text{mol/l}$ = 50 ng/ml), which is close to plasma concentration of verapamil after a 5-mg bolus injection (below 200 ng/ml).

Acknowledgments

The authors thank Drs. Charles Antzelevitch and Masahiko Kondo for their helpful suggestions and technical instructions, and Drs. Hans-J. Lang and Jürgen Pünter (Aventis Pharma Deutschland GmbH, Frankfurt, Germany) for kindly providing the chromanol 293B.

Reprint requests and correspondence: Dr. Wataru Shimizu, Division of Cardiology, Department of Internal Medicine, National Cardiovascular Center, 5-7-1 Fujishiro-dai, Suita, Osaka, 565-8565 Japan. E-mail: wshimizu@hsp.ncvc.go.jp.

REFERENCES

- Schwartz PJ, Periti M, Malliani A. The long Q-T syndrome. *Am Heart J* 1975;89:378-90.
- Moss AJ, Schwartz PJ, Crampton RS, et al. The long QT syndrome: prospective longitudinal study of 328 families. *Circulation* 1991;84:1136-44.
- Roden DM, Lazzara R, Rosen M, et al. Multiple mechanisms in the long-QT syndrome: current knowledge, gaps and future directions. *Circulation* 1996;94:1996-2012.
- Yang P, Kanki H, Drolet B, et al. Allelic variants in long-QT disease genes in patients with drug-associated Torsades de Pointes. *Circulation* 2002;105:1943-8.
- Donger C, Denjoy I, Berthet M, et al. KVLQT1 c-terminal missense mutation causes a forme fruste long-QT syndrome. *Circulation* 1997;96:2778-81.
- Napolitano C, Schwartz PJ, Brown AM, et al. Evidence for a cardiac ion channel mutation underlying drug-induced QT prolongation and life-threatening arrhythmias. *J Cardiovasc Electrophysiol* 2000;11:691-6.
- Kubota T, Shimizu W, Kamakura S, et al. Hypokalemia-induced long QT syndrome with underlying novel missense mutation in S4-S5 linker of KCNQ1. *J Cardiovasc Electrophysiol* 2000;11:1048-54.
- Cosio FG, Goicolea A, López-Gil L, Kallmeter C, Barroso L. Suppression of Torsades de Pointes with verapamil in patients with atrio-ventricular block. *Eur Heart J* 1991;12:635-8.
- Shimizu W, Ohe T, Kurita T, et al. Effects of verapamil and propranolol on early afterdepolarizations and ventricular arrhythmias induced by epinephrine in congenital long QT syndrome. *J Am Coll Cardiol* 1995;26:1299-309.
- Aiba T, Shimizu W, Inagaki M, et al. Transmural heterogeneity of the action potential configuration in the feline left ventricle. *Circ J* 2003;67:449-54.
- Antzelevitch C, Sun ZQ, Zhang ZQ, Yan GX. Cellular and ionic mechanisms underlying erythromycin-induced long QT intervals and Torsade de Pointes. *J Am Coll Cardiol* 1996;28:1836-48.
- Shimizu W, Antzelevitch C. Sodium channel block with mexiletine is effective in reducing transmural dispersion of repolarization and preventing Torsade de Pointes in LQT2 and LQT3 models of the long-QT syndrome. *Circulation* 1997;96:2038-47.
- Shimizu W, Antzelevitch C. Effects of a K⁺ channel opener to reduce transmural dispersion of repolarization and prevent Torsade de Pointes in LQT1, LQT2, and LQT3 models of the long-QT syndrome. *Circulation* 2000;102:706-12.
- Emori T, Antzelevitch C. Cellular basis for complex T wave and arrhythmic activity following combined I_{Kr} and I_{Ks} block. *J Cardiovasc Electrophysiol* 2001;12:1369-78.
- Yan GX, Wu Y, Liu T, et al. Phase 2 early afterdepolarization as a trigger of polymorphic ventricular tachycardia in acquired long-QT syndrome, direct evidence from intracellular recordings in the intact left ventricular wall. *Circulation* 2001;103:2851-6.
- Hamill OP, Marty A, Neher E, Sakmann B, Sigworth FJ. Improved patch-clamp techniques for high-resolution current recording from cells and cell-free membrane patches. *Pflügers Arch* 1981;391:85-100.
- Benitah JP, Gomez AM, Bailly P, et al. Heterogeneity of the early outward current in ventricular cells isolated from normal and hypertrophied rat hearts. *J Physiol* 1993;469:111-38.
- Clancy CE, Rudy Y. Na⁺ channel mutation that causes both Brugada and long-QT syndrome phenotypes, a simulation study of mechanism. *Circulation* 2002;105:1208-13.
- Dumaine R, Towbin JA, Brugada P, et al. Ionic mechanisms responsible for the electrocardiographic phenotype of the Brugada syndrome are temperature dependent. *Circ Res* 1999;85:803-9.
- Roden DM. Taking the "idio" out of "idiosyncratic": predicting Torsades de Pointes. *Pacing Clin Electrophysiol* 1998;21:1029-34.
- Vos MA, Verduyn SC, Gorgels APM, et al. Reproducible induction of early afterdepolarizations and Torsade de Pointes arrhythmias by d-sotalol and pacing in dogs with chronic atrioventricular block. *Circulation* 1995;91:864-72.
- Vos MA, Groot SHM, Verduyn SC, et al. Enhanced susceptibility for acquired Torsade de Pointes arrhythmias in the dog with chronic, complete AV block is related to cardiac hypertrophy and electrical remodeling. *Circulation* 1998;98:1125-35.
- Volders PGA, Sipido KR, Vos MA, et al. Downregulation of delayed rectifier K⁺ currents in dogs with chronic complete atrioventricular block and acquired Torsades de Pointes. *Circulation* 1999;100:2455-61.
- Burashnikov A, Antzelevitch C. Prominent I_{Kr} in epicardium and endocardium contributes to development of transmural dispersion of repolarization but protects against development of early afterdepolarizations. *J Cardiovasc Electrophysiol* 2002;13:172-7.
- Follmer CH, Colatsky TJ. Block of delayed rectifier potassium current, I_{Kr}, by flecainide and E-4031 in cat ventricular myocytes. *Circulation* 1990;82:289-93.
- Martínez HB, Elizalde A, Chapula JS. Developmental differences in delayed rectifying outward current in feline ventricular myocytes. *Am J Physiol* 2000;278:H484-92.
- January CT, Riddle JM. Early afterdepolarizations: mechanism of induction and block, a role for L-type Ca²⁺ current. *Circ Res* 1989;64:977-90.
- Luo CH, Rudy Y. A dynamic model of the cardiac ventricular action potential II afterdepolarizations, triggered activity, and potentiation. *Circ Res* 1994;74:1097-113.
- Bányász T, Fülöp L, Magyar J, et al. Endocardial versus epicardial differences in L-type calcium current in canine ventricular myocytes studied by action potential voltage clamp. *Cardiovasc Res* 2003;58:66-75.
- Cordeiro JM, Greene L, Heilmann C, Antzelevitch D, Antzelevitch C. Transmural heterogeneity of calcium activity and mechanical function in the canine left ventricle. *Am J Physiol* 2004;286:H1471-9.
- Greenstein JL, Wu R, Po S, et al. Role of the calcium-independent transient outward current I_{to1} in shaping action potential morphology and duration. *Circ Res* 2000;87:1026-33.
- Miyoshi S, Mitamura H, Fujikawa K, et al. A mathematical model of phase 2 reentry: role of L-type Ca current. *Am J Physiol* 2003;284:H1285-94.
- Furukawa T, Myerburg RJ, Furukawa N, et al. Differences in transient outward currents of feline endocardial and epicardial myocytes. *Circ Res* 1990;67:1287-91.
- Zygmunt AC, Goodrow RJ, Antzelevitch C. I_{NaCa} contributes to electrical heterogeneity within the canine ventricle. *Am J Physiol* 2000;278:H1671-8.
- Sanguinetti MC, Jurkiewicz NK, Scott A, Siegl PKS. Isoproterenol antagonizes prolongation of refractory period by class III antiarrhythmic agent E-4031 in guinea pig myocytes, mechanism of action. *Circ Res* 1991;68:77-84.
- Kimura S, Bassett AL, Xi H, Myerburg RJ. Early afterdepolarizations and triggered activity induced by cocaine, a possible mechanism of cocaine arrhythmogenesis. *Circulation* 1992;85:2227-35.

Pronounced HR variability after exercise in inferior ischemia: evidence that the cardioinhibitory vagal reflex is invoked by exercise-induced inferior ischemia

Nobuhiro Tahara,¹ Hiroshi Takaki,² Atsushi Taguchi,¹ Kazuhiro Suyama,¹ Takashi Kurita,¹ Wataru Shimizu,¹ Shunichi Miyazaki,¹ Toru Kawada,² and Kenji Sunagawa²

¹Division of Cardiology, Department of Medicine, National Cardiovascular Center, and ²Department of Cardiovascular Dynamics, National Cardiovascular Center Research Institute, Osaka, Japan

Submitted 22 January 2004; accepted in final form 19 October 2004

Tahara, Nobuhiro, Hiroshi Takaki, Atsushi Taguchi, Kazuhiro Suyama, Takashi Kurita, Wataru Shimizu, Shunichi Miyazaki, Toru Kawada, and Kenji Sunagawa. Pronounced HR variability after exercise in inferior ischemia: evidence that the cardioinhibitory vagal reflex is invoked by exercise-induced inferior ischemia. *Am J Physiol Heart Circ Physiol* 288: H1179–H1185, 2005. First published October 21, 2004; doi:10.1152/ajpheart.00045.2004.—Potent cardioinhibitory vagal reflex resulting in bradycardia and hypotension has been observed under particular conditions of transmural inferior ischemia and its reperfusion, such as those observed with acute infarction. However, whether exercise-induced ischemia with ST depressions that is subendocardial and that might be recurrently experienced in daily activities can evoke this reflex remains unknown. In patients with exercise-induced ST depressions due to either inferior [right coronary artery stenosis (RCA), $n = 52$] or anterior ischemia [left anterior descending artery stenosis (LAD), $n = 51$], we evaluated postexercise vagal activity (from 0 to 6 min) by the time constant of heart rate (HR) decay and HR variability by 30-s averages of the absolute values of successive RR interval differences (ΔRR). Exercise parameters were similar between groups. The time constant was slightly but significantly shorter in RCA than LAD patients (79 ± 24 vs. 93 ± 29 s, $P < 0.01$). More significantly, ΔRR early after exercise (0.5–2.5 min) was approximately twofold greater in RCA than LAD patients (from +76 to +118%, $P < 0.001$), indicating pronounced vagal activity stimulated by inferior ischemia. Revascularization prolonged the time constant ($P < 0.05$) and attenuated recovery ΔRR in RCA patients ($P < 0.05$, $n = 10$) but did not change both parameters in LAD patients ($n = 12$). As well as acute inferior infarction, exercise-induced inferior subendocardial ischemia, which might recurrently occur in daily activities, activates the cardioinhibitory reflex. These new findings must be taken into account in interpreting vagal activity in patients with coronary artery disease.

heart rate variability; vagus nerve; coronary artery disease

EXPERIMENTAL STUDIES in animals have demonstrated that excitation of vagal sensory nerve endings from myocardial ischemia involving the inferoposterior wall of the left ventricle activates potent cardioinhibitory reflex resulting in bradycardia and hypotension (7, 24). In humans, similar observations have been made under particular conditions of severe transmural inferior ischemia and its reperfusion, such as those that occur with myocardial infarction, vasospastic angina, or angioplasty of the right coronary artery (12, 15, 21, 22, 28). For example, in the first hour of the onset of acute myocardial infarction, patients with inferior infarction often (~75%) show sinus bradycardia and/or hypotension, which generally responds to

intravenous administration of atropine. This observation contrasts with that in patients with anterior infarction, about 50% of whom show sinus tachycardia and/or hypertension (15).

Despite these well-recognized clinical observations, little attention has been paid to the question as to whether this reflex could be evoked by exercise-induced ischemia that is usually subendocardial with the manifestation of ST depressions and that might be recurrently experienced during daily activities. If it does occur in this condition, this hitherto-unrecognized possibility must be taken into account in the clinical interpretation of vagal activity in patients with coronary artery disease (CAD). It is widely accepted that the higher the estimated measure of vagal activity, the better the patient status and the prognosis according to various reports examining the clinical significance of estimating vagal activity with the use of heart rate (HR) variability (HRV) analysis from 24-h Holter recording (1, 11, 13, 23a) or HR recovery after exercise testing (5, 18, 26). It is possible that vagal activity may be adversely augmented under a certain pathological condition, i.e., in the presence of inducible inferior ischemia, and that vagal estimation may be erroneously interpreted in patients with inducible inferior ischemia. In view of the diagnostic utility of exercise testing, the identification of the pronounced vagal activity induced by exercise may serve as an additive measure for detecting and localizing the presence of inferior ischemia.

On the basis of these considerations, the present study was designed to test the hypothesis that inferior ischemia, even that evoked by physiological stress such as exercise, may invoke the cardioinhibitory reflex, which would in turn influence postexercise HR decay and HRV through a reflex enhancement of vagal activity. The postexercise condition may more readily unmask this phenomenon than during exercise, because vagal activity is physiologically depressed during exercise but markedly reactivated after exercise (2, 20), although this reflex should be activated both during exercise-induced ischemia and after postexercise reperfusion. Thus we compared HR decay and HRV after exercise in patients with exercise-induced inferior ischemia and those with anterior ischemia and then evaluated the effects of revascularization on these parameters.

METHODS

Study population. From consecutive patients who underwent both coronary angiography and conventional treadmill exercise ECG testing within 3 wk for the evaluation of CAD, a total of 103 patients who were documented to have either inducible inferior ischemia due to

Address for reprint requests and other correspondence: H. Takaki, Dept. of Cardiovascular Dynamics, National Cardiovascular Center Research Institute, 5-7-1 Fujishiro-dai, Suita, Osaka 565-8565, Japan (E-mail: htakaki@res.ncvc.go.jp).

The costs of publication of this article were defrayed in part by the payment of page charges. The article must therefore be hereby marked "advertisement" in accordance with 18 U.S.C. Section 1734 solely to indicate this fact.

Table 1. Patient characteristics

	RCA	LAD
<i>n</i>	52	51
Age, yr	60 ± 10	63 ± 8
Men/women, <i>n</i>	45/7 (87/13)	45/6 (88/12)
Previous MI, <i>n</i>	25 (48)	26 (51)
LVEF, %	53 ± 11	52 ± 9
Hypertension, <i>n</i>	30 (58)	28 (55)
Diabetes mellitus, <i>n</i>	16 (31)	18 (35)
Medication		
β-Blockers, <i>n</i>	21 (40)	23 (45)
Ca antagonists, <i>n</i>	30 (58)	33 (65)
Nitrates, <i>n</i>	34 (65)	30 (59)

Values are means ± SD; *n*, no. of subjects. Values in parentheses are percentages. RCA, right coronary artery stenosis; LAD, left anterior descending coronary artery stenosis; MI, myocardial infarction; LVEF, left ventricular ejection fraction by contrast left ventriculography.

right coronary artery (RCA) stenosis (*n* = 52, RCA group) or anterior ischemia due to left anterior descending artery (LAD) stenosis (*n* = 51, LAD group) were enrolled in the study in a prospective fashion (Table 1). Significant coronary stenosis was defined as >50% luminal narrowing. All had significant exercise-induced ST segment depressions on treadmill ECG. Fifty-one (50%) patients had previous myocardial infarction. The majority (75%) had a single-vessel disease of either RCA stenosis (69%) or LAD stenosis (84%). In 24 patients with multiple vessel disease, exercise single-photon emission computed tomographic thallium-201 scintigraphy was performed to confirm that exercise-inducible ischemia was exclusively localized to either the inferior or anterior wall of the left ventricle. Exclusion criteria included the presence of atrial fibrillation, frequent premature beats (>5 beats/min) during the exercise test, and exercise-induced ST segment elevations (≥1.0 mm).

Clinical characteristics, including age, sex, prevalence of prior infarction, left ventricular ejection fraction (by contrast left ventriculography), and drug regimens, were quite similar between the two groups (Table 1). β-Blockers, calcium antagonists, and nitrates were taken in 44 (43%), 63 (61%), and 64 (62%) patients, respectively. No patient was taking digitalis at the time of the study. Drug regimens were neither altered nor stopped for the exercise test. The study protocol was approved by the ethics committee of our institution. All patients gave informed consent to participate in the study.

Exercise test. Conventional symptom-limited or submaximal (up to 90% age-predicted maximum HR) graded treadmill exercise testing was performed using a commercially available treadmill system (Formula; Esaote, Italy) equipped with an analog-to-digital converter and hard disk according to our protocol (23), being similar to the modified Bruce protocol. ECGs in lead V₂, aV_F, and V₅ were continuously monitored from rest through the recovery period. Arterial blood pressure was measured at rest, at the end of each stage, peak exercise, and at 1, 2, 4, and 6 min after exercise by a sphygmomanometer. Throughout the test, eight leads of the ECG, including lead I, II, and V₁₋₆, were continuously digitized at 500 Hz (12 bit) and stored on a computer hard disk for subsequent analysis. The standard 12-lead ECGs were hardcopied at rest, at the end of each stage, at peak exercise, immediately after exercise, and at every minute of the recovery period. A significant ST segment depression was defined by the following criteria: 1) a horizontal or downsloping ST segment displacement at J point ≥ 0.1 mV and 2) an upsloping ST segment displacement at 80 ms after J point ≥ 0.15 mV in at least three consecutive beats at peak exercise.

Assessment of revascularization effects. In 22 patients who subsequently received successful revascularization, we repeated the exercise test within 1 mo after the procedure. Eighteen patients received successful percutaneous transluminal coronary angioplasty either on

the RCA (*n* = 8) or LAD (*n* = 10). Coronary artery bypass graft surgery was undertaken in the other four patients (RCA *n* = 2, LAD *n* = 2).

On the basis of consideration that a higher attainment of peak HR resulting from increased exercise capacity after the intervention (i.e., different exercise time) and its possible influences on vagal activity would make it difficult to estimate the true effect of revascularization on postexercise HR analysis, the exercise test after revascularization was terminated at the same exercise duration as that before the revascularization. Drug regimens were also kept constant.

Data analysis. Off-line analysis was performed on a personal computer using our custom-made software. We first determined the beat-by-beat RR intervals throughout the test from rest to recovery period by detecting the peak of R wave deflections. In patients with premature beats, we corrected RR intervals by linear interpolation with the previous and following beats.

Using the time series of RR intervals during recovery periods of 6 min, we computed the time constant of HR decay. We fitted the HR data to a monoexponential curve ($HR = A + Be^{-t/\tau}$, where *A* and *B* are constants, *t* is the elapsed time after peak exercise, and τ is the time constant of recovery) by nonlinear least-squares regression analysis. We then estimated the time course of HRV by time-domain and frequency-domain analysis as follows. Instead of parameters such as the standard deviation of the average interval between normal beats, which is substantially influenced by dynamic changes in overall trend, serial changes in HRV were assessed by 30-s averages of the absolute values of successive beat-to-beat differences in the RR interval (ΔRR). Serial changes in HRV were also evaluated by 30-s averages of the beat-to-beat percent changes [absolute successive differences relative to instantaneous RR interval (% ΔRR)] to eliminate the effect of the individual variation in HR.

Power spectral analysis of RR interval changes was also performed by fast Fourier transformation. We serially computed the spectrum of RR interval data of 1-min duration with 50% overlapping of each segment (0–1 min, 0.5–1.5 min, . . . , 4.5–5.5 min, 5–6 min; 11 segments in all). The linear trend in the data was subtracted from the data set in each segment. A Blackman-Harris window was applied to reduce spectral leakage.

Statistical analysis. Data are presented as means ± SD. Serial changes in variables were evaluated by repeated-measures ANOVA followed by Scheffé's test for intergroup and intragroup comparisons. Student's unpaired and paired *t*-tests, linear regression analysis, multiple linear regression analysis, and χ^2 -analysis were used when applicable. A *P* value of <0.05 was considered statistically significant.

RESULTS

All exercise tests were completed without any unfavorable events or serious complications. Exercise test parameters including exercise duration, resting and peak HR, resting and peak systolic blood pressure, the maximum magnitude of ST segment depression, and the occurrence of exercise-induced angina were consistently similar between the RCA and LAD groups (Table 2). Only peak HR tended to be lower in the RCA

Table 2. Exercise test results

	RCA	LAD
Exercise time, s	507 ± 159	497 ± 133
HR, beats/min		
Resting	65 ± 12	65 ± 11
Peak	126 ± 22	135 ± 21
SBP, mmHg		
Resting	129 ± 13	130 ± 18
Peak	158 ± 24	160 ± 20
ST depression, mm	-2.0 ± 0.8	-1.7 ± 1.5
Angina, <i>n</i>	22/30	25/26

Values are means ± SD. HR, heart rate; SBP, systolic blood pressure; *n*, no. of subjects.

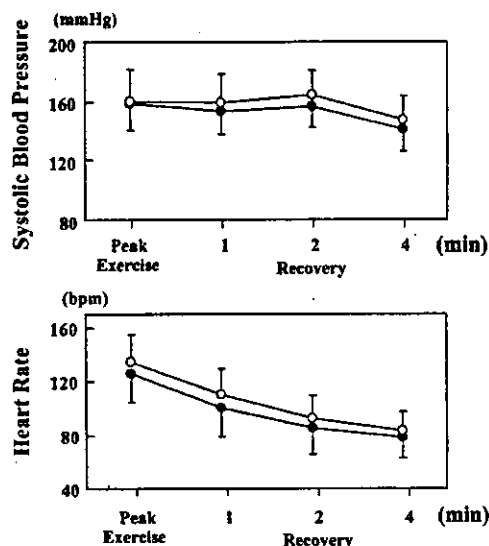


Fig. 1. Time course of systolic blood pressure (*top*) and heart rate [HR, in beats/min (bpm); *bottom*] in right coronary artery (RCA) stenosis (closed circles) and left anterior descending artery (LAD) stenosis (open circles) patients. No differences were observed in either parameter. Values are expressed as means \pm SD.

group (126 ± 22 beats/min) than in the LAD group (135 ± 21 beats/min), but this difference did not reach statistical significance.

Postexercise systolic blood pressure and HR. There was no significant difference between the groups with respect to postexercise systolic blood pressure and HR at 1, 2, and 4 min of recovery (Fig. 1).

Postexercise HR decay and HRV. Shown in Fig. 2 are representative examples of the time series of beat-by-beat HR and absolute value of the successive RR interval changes throughout the exercise test. A patient with RCA stenosis (Fig. 2, *left*) showed a transient increase in RR variability soon after the termination of exercise, whereas such findings were not observed in a patient with LAD stenosis (Fig. 2, *right*). The time constant was shorter in the former (92 s) than in the latter (112 s).

When pooled data were compared between the two groups, the time constant of postexercise HR decay was slightly but

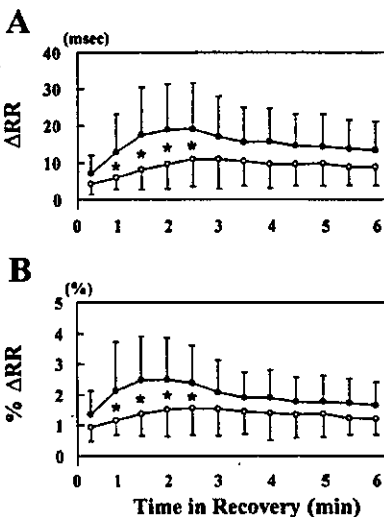
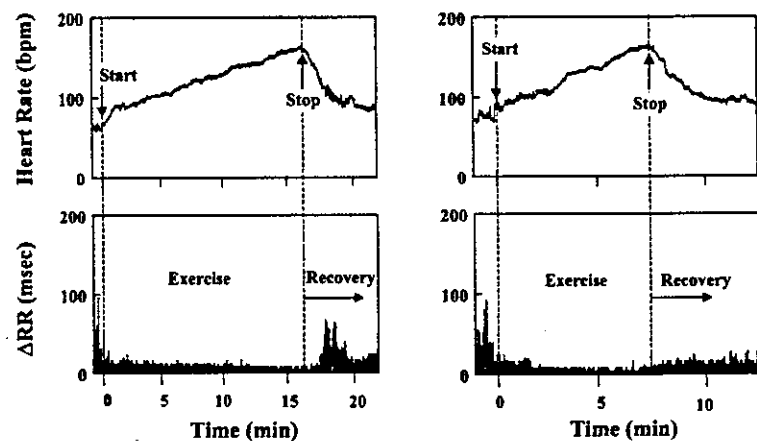


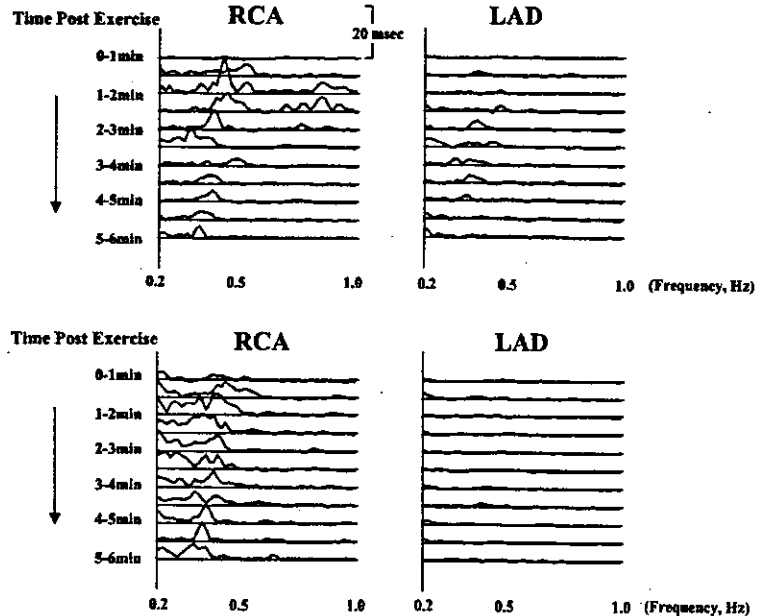
Fig. 3. Comparisons of the HRV time course expressed by ΔRR (A) and absolute successive differences relative to instantaneous RR interval (% ΔRR ; B). Closed circles depict the RCA stenosis group, and open circles depict the LAD stenosis group. Values are expressed as means \pm SD. * $P < 0.01$, RCA stenosis patients vs. LAD stenosis patients.

significantly shorter in RCA than LAD patients (79 ± 24 vs. 93 ± 29 s, $P < 0.01$). More significantly, postexercise HRV expressed by ΔRR (average over every 30 s) early after exercise was markedly greater in RCA than LAD patients for a period of 1.0–2.5 min ($P < 0.001$ for all; Fig. 3A). % ΔRR was similarly greater in RCA patients than in LAD patients in the same period of 1.0–2.5 min after exercise ($P < 0.001$ for 1.0–2.0 min and $P < 0.01$ for 2.5 min; Fig. 3B).

Figure 4, *top*, shows serial changes in the power spectrum of RR intervals in the recovery period analyzed in the same two patients shown in Fig. 2. As can be seen, unlike the patient with LAD stenosis (Fig. 4, *right*), the patient with RCA stenosis (Fig. 4, *left*) showed substantial amounts of power spectra in the frequency range between ~ 0.30 and 0.60 Hz. When these data were pooled (Fig. 4, *bottom*), total power within the frequency range between 0.25 and 0.60 Hz (corresponding to the respiratory rates after exercise) was significantly higher in the RCA group than in the LAD group in the four time window segments early after exercise, i.e., 0.5–1.5 min, 1.0–2.0 min,

Fig. 2. Representative trends of beat-by-beat HR (*top*) and absolute values of successive beat-to-beat differences in the RR interval (ΔRR ; *bottom*) from rest to recovery in a patient with RCA stenosis (*left*) and in a patient with LAD stenosis (*right*). A transient increase in HR variability (HRV) can be seen soon after exercise in the patient with RCA stenosis.

Fig. 4. Top: representative data of power spectrum analysis of HRV obtained in the same 2 patients shown in Fig. 2 (left, RCA stenosis patient; right, LAD stenosis patient). Horizontal lines depict the frequency (in Hz). The data series of power spectrum for 1 min are shown serially from the top (0–1 min) downward with time of recovery (overlapping 30 s). The spectral component of RR intervals for each segment is shown as the square root of the power (i.e., amplitude). Bottom: pooled data of power spectrum analysis in the RCA stenosis group (left; $n = 52$) and LAD stenosis group (right; $n = 51$).



1.5–2.5 min, and 2.0–3.0 min ($P < 0.005$ for the first 3 segments and $P < 0.02$ for 2.0- to 3.0-min segment).

Figure 5 shows scatterplots of ΔRR at 1.5 min (60–90 s) versus the time constant for all patients. There was a relatively close relationship ($r = -0.50$, $P < 0.001$) between these parameters. When ΔRR at 1.5 min (60–90 s) for each patient was plotted separately in RCA and LAD patients (Fig. 6), the prevalence of pronounced HRV (exceeding 12 ms) was much more frequently found in RCA patients (58%) than in LAD patients (16%, $P < 0.001$). Subgroup analysis of RCA patients showed that those with enhanced HRV were significantly younger (58 ± 11 vs. 64 ± 8 yr, $P < 0.01$) and had a significantly lower HR at rest (61 ± 10 vs. 70 ± 12 beats/min, $P < 0.01$) and peak HR (117 ± 19 vs. 139 ± 18 beats/min, $P < 0.01$) compared with those without this phenomenon.

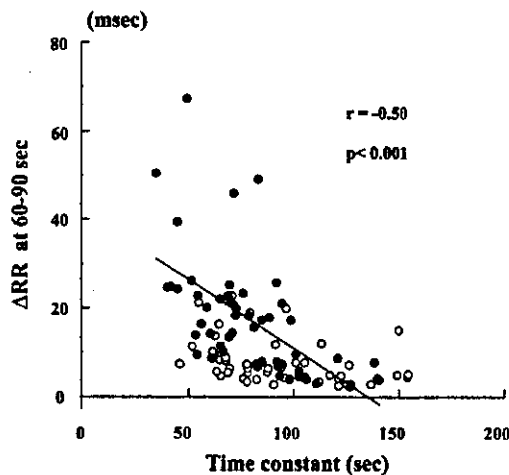


Fig. 5. Graph showing the relationship between ΔRR (60–90 s) and the time constant. Closed circles, RCA stenosis patient; open circles, LAD stenosis patient.

There was no significant difference with respect to sex, left ventricular ejection fraction, the use of cardiovascular drugs (β -blockers, calcium antagonists, or nitrates), prevalence of previous myocardial infarction, history of diabetes mellitus, exercise time, magnitude of ST depression, occurrence of exercise-induced angina, or resting ΔRR level. When multiple linear regression analysis that included clinical, angiographic, and exercise variables was used in the overall population, age ($P = 0.02$), resting HR ($P = 0.04$), and peak exercise HR ($P = 0.02$) together with the location of ischemia ($P < 0.0001$) were independently associated with ΔRR (60–90 s).

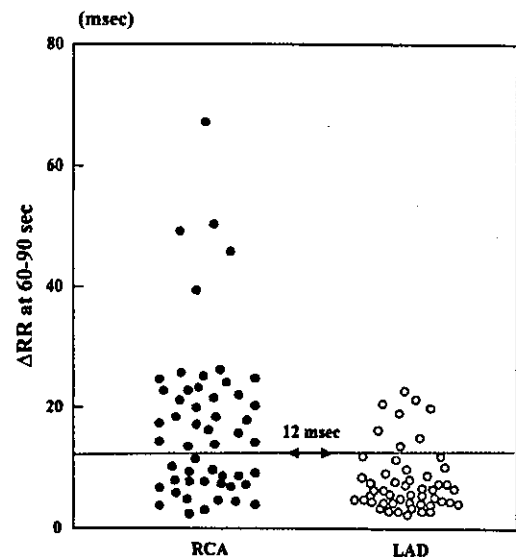


Fig. 6. Scatterplots of ΔRR at 60–90 s plotted separately for each patient in the RCA (left) and LAD (right) stenosis groups. Pronounced HRV (defined as $\Delta RR > 12$ ms; dotted line) was observed in 58% of RCA stenosis patients, whereas it was found in 16% of LAD stenosis patients ($P < 0.001$).

Effects of revascularization on postexercise HR decay and HRV. In either the RCA or LAD patient group, HR at both rest and the end of exercise were not significantly different before and after revascularization (note that the second test was terminated at the same duration as was achieved at the first test). In RCA patients, HR at 1 and 2 min of recovery were significantly higher (both $P < 0.05$) after than before revascularization, whereas no such significant differences were observed in LAD patients.

After revascularization, in RCA patients, ΔRR early after exercise was significantly attenuated (from 22 ± 14 to 9 ± 5 ms for 60–90 s, from 25 ± 12 to 11 ± 5 ms for 90–120 s, and from 27 ± 13 to 13 ± 5 ms for 120–150 s, all $P < 0.05$; Fig. 7). The time constant was concordantly prolonged (from 73 ± 21 to 96 ± 30 s, $P < 0.05$). Both parameters in RCA patients changed toward the same level as those in LAD patients, in whom both parameters remained unchanged after the revascularization procedure. There was no significant difference in systolic blood pressure at any time point in both RCA and LAD patient groups.

DISCUSSION

Although potent cardioinhibitory vagal reflex stimulated by inferior ischemia (the so-called Bezold-Jarisch reflex) has been recognized under particular conditions of transmural ischemia in animal and human studies (7, 12, 15, 21, 22, 24, 28), whether exercise-induced transient subendocardial ischemia could evoke this reflex has received little attention and has not been previously examined. The present study indicated that exercise-induced inferior ischemia with ST depressions reflecting subendocardial ischemia, which might be recurrently experienced in daily activities, activates the cardioinhibitory reflex as evidenced by a faster postexercise HR decay and more pronounced HRV in RCA patients compared with LAD patients. In addition, removal of inferior ischemia by revascularization prolonged the time constant and reduced pronounced HRV in the early recovery in RCA patients, whereas revascularization did not significantly change these parameters in LAD patients. These findings, indicative of the direct role of “localized inferior ischemia” on the appearance of this phenomenon, support the validity of our hypothesis that transmural severe ischemia is not a prerequisite for the manifestation of this reflex.

Estimation of vagal activity. Numerous previous studies have indicated the clinical importance of estimating the vagal activity regulating the cardiovascular system in patients with

heart disease by noninvasive methods such as HRV analysis (1, 11, 13, 23a) and baroreflex sensitivity measurements with phenylephrine injection (3, 13, 14). After a report of Imai et al. (10) demonstrating that the rate of HR decay after exercise is a function of the reactivation of vagal activity, recent studies have shown the postexercise HR fall is a useful marker for predicting mortality in subjects with suspected CAD (5, 18, 26). In the present study, to assess the dynamic changes in vagal activity, serial HRV analysis during recovery was conducted by calculating ΔRR and $\% \Delta RR$ every 30 s along with the evaluation of the HR decay (time constant). As a result, both HRV parameters in RCA patients markedly increased from 0.5 to 1 min of recovery, remained rather constant up to 2.5 min, and thereafter decreased nearly to the level of those in LAD patients. The group difference was more striking compared with that of the time constant. The characteristic overshooting of the HRV parameters suggests a transiently enhanced vagal activity as a “reperfusion reflex” after the resolution of exercise-induced ischemia. In agreement with its observed time course, frequency analysis also revealed a transient augmentation of power spectrum of RR intervals in high-frequency ranges early after exercise, supporting the validity of reperfusion-stimulated vagal overactivation.

It should be of importance that, in the present study, the exercise duration after revascularization was matched to that before the procedure. This is because a higher level of exercise intensity, as a consequence of the removal of critical stenosis, would alter the postexercise autonomic activity, possibly making it difficult to estimate the direct effects of revascularization.

Cardioinhibitory reflex activated by exercise-induced ischemia. To the best of our knowledge, no previous study has been systematically conducted to evaluate the possible role of exercise-induced ischemia with ST depressions on this reflex phenomenon. Miller et al. (16) reported on seven patients who developed sinus deceleration during exercise testing, all of whom had angiographically documented RCA lesions. The authors speculated the role of Bezold-Jarisch reflex in this mechanism and stated that the prevalence of deceleration during exercise appears to be very low, which is in agreement with our experiences in the exercise laboratory. Sinus deceleration during exercise may be an extreme example caused by an ischemia-mediated reflex (4, 6).

Thus this reflex phenomenon is presumably operative during exercise-induced ischemia as well as during postexercise reperfusion; however, we focused on postexercise HR dynamics for the following reasons. Because vagal activity is physiologi-

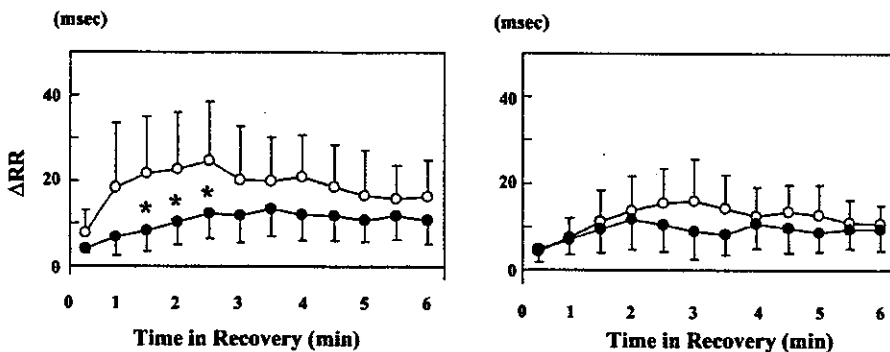


Fig. 7. Changes in the HRV (ΔRR) time course after revascularization in the RCA (left; $n = 52$) and LAD (right; $n = 51$) stenosis groups. Open circles depict the values before the procedure, and closed circles depict the values after the procedure. Values are expressed as means \pm SD. * $P < 0.05$, before vs. after revascularization.



cally attenuated in proportion to the increase in exercise intensity, this reflex might be masked during exercise. In contrast, potent reactivation of vagal nerve activity after exercise may accelerate the appearance of this reflex under a higher vagal condition after exercise. In practice, several cases among RCA patients showed a pronounced HRV and marked impairment of HR increase even during exercise indicative of the operation of this reflex during exercise; however, we also found a markedly rapid HR decay and more profound increase in HRV during recovery almost without exception.

The physiological implication of this reflex, namely, what role this reflex may play, is unknown. The possibility that the reflex cardioprotectively works thorough the reduction in myocardial oxygen demand or that the resultant high vagal tone prevents the development of serious ventricular arrhythmias is of interest (9, 19); however, there are few available data to support this so far.

Pronounced HRV after exercise (defined as $\Delta RR > 12$ ms) was observed in 58% of RCA patients but in only 16% of LAD patients. These prevalences are very similar to those during the observation of the "bradycardia-hypotension" pattern observed in patients early after acute inferior and anterior myocardial infarction, respectively (27). The difference probably indicates that the vagal nerves involving this reflex are preferentially distributed in the inferior area but some mounts of fibers are distributed in the anterior area of the left ventricle.

In RCA patients, none of the clinical, angiographic, and exercise parameters differed between patients with and without this phenomenon except in regard to age, resting HR, and peak HR. All of these three parameters were independently associated with HRV early after exercise in our multiple regression analysis. Vagal activity is known to be strongly associated with age and resting HR. Thus it is suggested that the presence or absence of this phenomenon would depend on the basal level of vagal activity rather than other parameters such as severity of ischemia or the presence of previous myocardial infarction.

Clinical implications. The findings demonstrated in the present study should provide a new insight into the interpretation of estimated vagal activity in patients with CAD. It is widely accepted that autonomic imbalance, i.e., vagal withdrawal and coexisting sympathetic activation, is associated with poor prognosis and pathophysiology in various types of heart disease (25). In other words, we believe that the higher the vagal activity, the better the patient prognosis and status. However, present data suggest that this is not necessarily the case in some patients under certain conditions. For example, studies using Holter recordings showed that a considerable number of patients with documented CAD frequently experience episodes of transient myocardial ischemia in their daily life (17). In such patients, transient enhancement of HRV provoked by inferior ischemia may often occur, leading to an erroneous interpretation of HRV. In addition, there are several studies (5, 18, 26) that related a poor prognosis to attenuated HR recovery after exercise testing on the assumption that a fall in HR recovery immediately after exercise is a function of vagal reactivation. These findings might be true in the overall population; however, it should be noted that a rapid HR decrease after exercise may occur under a pathological condition through an ischemia-mediated cardioinhibitory reflex. HRV measures might be affected not by the patient status but by the presence of inferior ischemia.

We did not analyze postexercise parameters in subjects without CAD. This is because they should be capable of exercising far longer than our patients with exercise-induced ischemia, which may considerably influence the postexercise vagal activity. At present, we can consider that the vagal overactivation after exercise may be useful in predicting the presence of inferior ischemia when significant exercise-induced ST depressions are observed. It may also be useful in patients after angioplasty of RCA disease to predict restenosis or to confirm the therapeutic effects.

Study limitations. It is generally considered that anterior ischemia is more deleterious than inferior ischemia in terms of hemodynamics, leading to a more severe autonomic impairment, i.e., a more depressed vagal activity in LAD patients. Thus the observed differences in vagal activity between the groups might be caused not only by the cardioinhibitory reflex evoked by inferior ischemia but also by the differences in hemodynamic impairment. For this reason, we evaluated the changes in vagal parameters (time constant and ΔRR) after revascularization and found that these parameters were significantly altered in RCA patients but not in LAD patients. This strongly supports the notion that the differences in estimated vagal activity between the groups are determined primarily by the presence or absence of inferior located ischemia. Nevertheless, we cannot completely exclude the possible contribution of the different sympathetic tone between the groups, because anterior located ischemia, although rare, can stimulate this reflex.

In conclusion, as well as transmural myocardial ischemia with ST elevations such as that occurring with acute inferior myocardial infarction, exercise-induced transient inferior sub-endocardial ischemia with ST depressions, which might be recurrently experienced in daily activities, activates cardioinhibitory reflex by stimulating vagal nerve endings in humans. This hitherto-unknown findings must be taken into account in the estimation of vagal function conducted in various clinical settings, especially when evaluating patients with CAD.

GRANTS

This study was supported by Ministry of Health and Welfare of Japan Research Grant for Cardiovascular Diseases 11C-7, by Japan Society for the Promotion of Science Grant-In-Aid for Scientific Research C-11670730, and by the Program for Promotion of Fundamental Studies in Health Science from the Organization for Pharmaceutical Safety and Research.

REFERENCES

1. Algra A, Tijssen JGP, Roelandt JRTC, Pool J, and Lubsen J. Heart rate variability from 24-hour electrocardiography and the 2-year risk for sudden death. *Circulation* 88: 180–185, 1993.
2. Arai Y, Saul JP, Albrecht P, Hartley LH, Lilly LS, Cohen RJ, and Colucci WS. Modulation of cardiac autonomic activity during and immediately after exercise. *Am J Physiol Heart Circ Physiol* 256: H132–H141, 1989.
3. Bigger JT Jr, La Rovere MT, Steinman RC, Fleiss JL, Rottman JN, Rolnitzky LM, and Schwartz PJ. Comparison of baroreflex sensitivity and heart period variability after myocardial infarction. *J Am Coll Cardiol* 14: 1511–1518, 1989.
4. Chokshi SK, Sarmiento J, Nazari J, Mattioni T, Zheutlin T, and Kehoe R. Exercise-provoked distal atrioventricular block. *Am J Cardiol* 66: 114–116, 1990.
5. Cole CR, Blackstone EH, Pashkow FJ, Snader CE, and Lauer MS. Heart rate recovery immediately after exercise as a predictor of mortality. *N Engl J Med* 341: 1351–1357, 1999.

6. Coplan NL, Morales MC, Romanello P, Wilentz JR, and Moses JW. Exercise-related atrioventricular block: influence of myocardial ischemia. *Chest* 100: 1728-1730, 1991.
7. Felder RB and Thames MD. Interaction between cardiac receptors and sinoaortic baroreceptors in the control of efferent cardiac sympathetic nerve activity during myocardial ischemia in dogs. *Circ Res* 45: 728-736, 1979.
9. Huikuri HV, Valkama JO, Airaksinen KEJ, Seppanen T, Kessler KM, Takkanen JT, and Myerburg RJ. Frequency domain measures of heart rate variability before the onset of nonsustained and sustained ventricular tachycardia in patients with coronary artery disease. *Circulation* 87: 1220-1228, 1993.
10. Imai K, Sato H, Hori M, Kusuoka H, Ozaki H, Yokoyama H, Takeda H, Inoue M, and Kamada T. Vagally mediated heart rate recovery after exercise is accelerated in athletes but blunted in patients with chronic heart failure. *J Am Coll Cardiol* 24: 1529-1535, 1994.
11. Kleiger RE, Miller JP, Bigger JT Jr, Moss AJ, and the Multicenter Postinfarction Research Group. Decreased heart rate variability and its association with increased mortality after acute myocardial infarction. *Am J Cardiol* 59: 256-262, 1987.
12. Koren G, Weiss AT, Ben-David Y, Hasin Y, Luria MH, and Gotsman MS. Bradycardia and hypotension following reperfusion with streptokinase (Bezold-Jarisch reflex): a sign of coronary thrombolysis and myocardial salvage. *Am Heart J* 112: 468-471, 1986.
13. La Rovere MT, Bigger JT Jr, Marcus FI, Mortana A, and Schwartz PJ for the Autonomic Tone and Reflexes After Myocardial Infarction Investigators. Baroreflex sensibility and heart-rate variability in prediction of total cardiac mortality after myocardial infarction. *Lancet* 351: 478-484, 1998.
14. La Rovere MT, Specchia G, Mortara A, and Schwartz PJ. Baroreflex sensitivity, clinical correlates, and cardiovascular mortality among patients with a first myocardial infarction: a prospective study. *Circulation* 78:816-824, 1988.
15. Mark AL. The Bezold-Jarisch reflex revisited: clinical implications of inhibitory reflexes originating in the heart. *J Am Coll Cardiol* 1: 90-102, 1983.
16. Miller TD, Gibbons RJ, Squires RW, Allison TG, and Gau GT. Sinus node deceleration during exercise as a marker of significant narrowing of the right coronary artery. *Am J Cardiol* 71: 371-373, 1993.
17. Mulcahy D, Husain S, Zalos G, Rehman A, Andrews NP, Schenke WH, Geller NL, and Quyyumi AA. Can ambulatory monitoring identify high-risk patients with stable coronary artery disease? *JAMA* 277: 318-324, 1997.
18. Nishime EO, Cole CR, Blackstone EH, Pashkow FJ, and Lauer MS. Heart rate recovery and treadmill exercise score as predictors of mortality in patients referred for exercise ECG. *JAMA* 284: 1392-1398, 2000.
19. Pedretti R, Etro MD, Laporta A, Braga SS, and Caru B. Prediction of late arrhythmic events after acute myocardial infarction from combined use of noninvasive prognostic variables and inducibility of sustained monomorphic ventricular tachycardia. *Am J Cardiol* 71: 1131-1141, 1993.
20. Perini R, Orizio C, Comandè A, Castellano M, Beschi M, and Veicsteinas A. Plasma norepinephrine and heart rate dynamics during recovery from submaximal exercise in man. *Eur J Appl Physiol* 58:879-883, 1989.
21. Prez-Gomez F, Martín de Dios R, Rey J, and Aguado AG. Prinzmetal's angina: reflex cardiovascular response during episode of pain. *Br Heart J* 42: 81-87, 1979.
22. Robertson RM and Robertson D. The Bezold-Jarisch reflex: possible role in limiting myocardial ischemia. *Clin Cardiol* 4: 75-79, 1981.
23. Sato I, Tomobuchi Y, Funahashi T, Ohe T, Kamakura S, Matsuhisa M, Haze K, and Shimomura K. Poor responsiveness of heart rate to treadmill exercise in vasospastic angina. *Clin Cardiol* 8: 206-212, 1985.
- 23a. Task Force of the European Society of Cardiology and the North American Society of Pacing and Electrophysiology. Heart rate variability: standards of measurement, physiology interpretation, and clinical use. *Circulation* 93: 1043-1065, 1996.
24. Thames MD, Klopfenstein HS, Abboud FM, Mark AL, and Walker JL. Preferential distribution of inhibitory cardiac receptors with vagal afferents to the inferoposterior wall of the left ventricle activated during coronary occlusion in the dog. *Circ Res* 43: 512-519, 1978.
25. Tsuji H, Larson MG, Venditti FJ, Manders ES, Evans JC, Feldman CL, and Levy D. Impact of reduced heart rate variability on risk for cardiac events: the Framingham Heart Study. *Circulation* 94: 2850-2855, 1996.
26. Watanabe J, Thamilarasan M, Blackstone EH, Thomas JD, and Lauer MS. Heart rate recovery immediately after treadmill exercise and left ventricular systolic dysfunction as predictors of mortality: the case of stress echocardiography. *Circulation* 104: 1911-1916, 2001.
27. Webb SW, Adgey AAJ, and Pantridge JF. Autonomic disturbance at onset of acute myocardial infarction. *Br Med J* 3: 89-92, 1972.
28. Wei JY, Markis JE, Malagold M, and Braunwald E. Cardiovascular reflexes stimulated by reperfusion of ischemic myocardium in acute myocardial infarction. *Circulation* 67: 796-801, 1983.

Bezold-Jarisch Reflex Blunts Arterial Baroreflex via the Shift of Neural Arc toward Lower Sympathetic Nerve Activity

K. KASHIHARA*†, T. KAWADA*, MEIHUA LI*†, M. SUGIMACHI*, and K. SUNAGAWA*

*Department of Cardiovascular Dynamics, National Cardiovascular Center Research Institute, 5-7-1 Fujishirodai, Suita, Osaka, 565-8565 Japan; and †Organization for Pharmaceutical Safety and Research, Shin-Kasumigaseki Bldg., 3-3-2 Kasumigaseki, Chiyoda, Tokyo, 100-0013 Japan

Abstract: Although the Bezold-Jarisch (BJ) reflex is potentially evoked during acute myocardial ischemia or infarction, its effects on the static characteristics of the arterial baroreflex remain to be analyzed in terms of an equilibrium diagram between the neural and peripheral arcs. The neural arc represents the static input-output relationship between baroreceptor pressure input and efferent sympathetic nerve activity (SNA), whereas the peripheral arc represents that between SNA and arterial pressure (AP). In 8 anesthetized rabbits, we increased carotid sinus pressure stepwise from 40 to 160 mmHg in increments of 20 mmHg at one-minute intervals while measuring renal SNA and AP under control conditions and during the activation of the BJ reflex by intravenous administration of

phenylbiguanide (PBG, 100 $\mu\text{g}\cdot\text{kg}^{-1}\cdot\text{min}^{-1}$). The neural arc approximated a sigmoid curve whereas the peripheral arc approximated a straight line. PBG decreased AP at the operating point from 91.3 ± 2.4 to 71.7 ± 3.1 mmHg ($P < 0.01$), and attenuated the total loop gain at the operating point from -1.31 ± 0.44 to -0.51 ± 0.14 ($P < 0.05$). The equilibrium diagram indicated that PBG caused a parallel shift of the neural arc toward lower SNA such that the maximum SNA was reduced to approximately 60% of control. PBG decreased neural and peripheral arc gains at the operating point to approximately 43% and 77%, respectively. In conclusion, the BJ reflex blunts arterial baroreflex via the shift of the neural arc toward lower SNA. [The Japanese Journal of Physiology 54: 395–404, 2004]

Key words: renal sympathetic nerve activity, carotid sinus baroreflex, equilibrium diagram analysis, phenylbiguanide, rabbits.

Intravenous injection of veratrum alkaloids in experimental animals induces inhibitory cardiorespiratory responses known as the Bezold-Jarisch reflex [1, 2]. The Bezold-Jarisch reflex is mediated by several types of cardiopulmonary receptors including serotonin 5-HT₃ receptors on the cardiopulmonary vagal afferent fibers [3–6]. Activations of the cardiopulmonary chemosensitive vagal afferent fibers reduces arterial pressure (AP), heart rate (HR), and cardiac output [7–9]. Therefore, the Bezold-Jarisch reflex could have a significant influence on circulatory reg-

ulation during acute myocardial ischemia or infarction where cardiac chemoreceptors are potentially activated [10, 11]. Although the physiological significance of this reflex remains debatable [12, 13], elucidating the effects of the Bezold-Jarisch reflex on circulatory regulation should contribute to the understanding of the pathophysiology underlying ischemic heart diseases. Because the arterial baroreflex system is a major negative feedback system that stabilizes AP against acute pressure disturbances, we aimed to clarify the effects of the Bezold-Jarisch

Received on July 8, 2004; accepted on August 20, 2004

Correspondence should be addressed to: Koji Kashihara, Department of Cardiovascular Dynamics, National Cardiovascular Center Research Institute, 5-7-1 Fujishirodai, Suita, Osaka, 565-8565 Japan. Phone: +81-6-6833-5012, Fax: +81-6-6835-5403, E-mail: kashihara@ri.ncvc.go.jp